Messinian vegetation and climate of the intermontane Florina-Ptolemais-Servia Basin, NW Greece inferred from palaeobotanical data: How well do plant fossils reflect past environments?

Johannes M. Bouchal[1*], Tuncay H. Güner[3], Dimitrios Velitzelos[3], Evangelos Velitzelos[3], Thomas Denk[4]

[1]Research group Aerobiology and pollen information, Department of Oto-Rhino-Laryngology, Medical University Vienna, Vienna, Austria
[2]Faculty of Forestry, Department of Forest Botany, Istanbul University Cerrahpaşa, Istanbul, Turkey
[3]National and Kapodistrian University of Athens, Faculty of Geology and Geoenvironment, Section of Historical Geology and Palaeontology, Greece
[4]Swedish Museum of Natural History, Department of Palaeobiology, Box 50007, 10405 Stockholm, Sweden

Abstract

The late Miocene is marked by pronounced environmental changes and the appearance of strong temperature and precipitation seasonality. Although environmental heterogeneity is to be expected during this time, it is challenging to reconstruct palaeoenvironments using plant fossils. We investigated leaves and dispersed spores/pollen from 6.4–6 Ma strata in the intermontane Florina-Ptolemais-Servia Basin (FPS) of northwestern Greece. To assess how well plant fossils reflect the actual vegetation of the FPS, we assigned fossil-taxa to biomes providing a measure for environmental heterogeneity. Additionally, the palynological assemblage was compared to pollen spectra from modern lake sediments to assess biases in spore/pollen representation in the pollen record. We found a close match of the Vegora assemblage with modern *Fagus–Abies* forests of Turkey. Using taxonomic affinities of leaf fossils, we further established close similarities of the Vegora assemblage with modern laurophyllous oak forests of Afghanistan. Finally, using information from sedimentary environment and taphonomy, we distinguished local and distantly growing vegetation types. We then subjected the plant assemblage of Vegora to different methods of climate reconstruction and discussed their potentials and limitations. Leaf and spore/pollen records allow accurate reconstructions of palaeoenvironments in the FPS, whereas extra-regional vegetation from coastal lowlands is likely not captured.

Keywords

Biome reconstruction, proxy biases, climate reconstruction, plant macrofossils, dispersed pollen, light and scanning electron microscopy

1. Introduction

The late Miocene (11.6–5.3 Ma) marks the time in the Neogene (23–2.58 Ma) with the largest shift from equable climate to strong latitudinal temperature gradients in both hemispheres (Herbert et al., 2016). This is well illustrated by the global rise of C_4 dominated ecosystems (grasslands and savannahs in the tropics and subtropics; Cerling et al., 1997). In the Mediterranean region, vegetation changes did not happen synchronously with modern steppe and Mediterranean sclerophyllous woodlands replacing humid temperate forest vegetation at different times and places during the middle and late Miocene (Suc, 1984; Kovar-Eder, 2003; Fauquette et al., 2006; Kovar-Eder et al., 2006; Bouchal et al., 2018; Denk et al., 2018; Suc et al., 2018). During the latest Miocene (5.9–5.3 Ma) the desiccation of the Mediterranean Sea was caused by its isolation from the Atlantic Ocean. Based on palynological studies across the Mediterranean region, this event did not have a strong effect on the existing vegetation. Open and dry environments existed in southern parts before, during, and after this so-called Messinian Salinity Crisis (MSC; Hsü et al., 1973). In contrast, forested vegetation occurred in northern parts of Spain, Italy, and the western Black Sea region (Fauquette et al., 2006). Likewise, a vegetation gradient occurred from North and Central Italy and Greece to Turkey, where humid temperate forests had disappeared by the early late Miocene (Denk et al., 2018). The Florina-Ptolemais-Servia Basin (FPS; Steenbrink et al., 2006) of northwestern Greece and its extensions to the north (Bitola Basin) and south (Likoudi Basin) is one of the best-understood intermontane basins of late Miocene age in the entire Mediterranean region. A great number of studies investigated the tectonic evolution, depositional history, and temporal constraints of basin fills (e.g. Steenbrink et al. 1999, 2000, 2006), plant fossils (e.g. Knobloch & Velitzelos, 1986a,b; Velitzelos & Gregor, 1985; Mai & Velitzelos, 1992; Kvaček et al.,

2002; Velitzelos et al., 2014), and vertebrate fossils (van de Weerd, 1979; Koufos, 1982, 2006; Koufos et al., 1991).

The Messinian flora of Vegora in the northern part of the FPS is dated at 6.4–6 Ma and represents the vegetation in this region just before the onset of the Messinian salinity crisis (the pre-evaporitic Messinian). This flora has been investigated since 1969 (Kvaček et al., 2002) and represents one of the richest late Miocene leaf floras in the eastern Mediterranean along with two other, slightly older, Messinian plant assemblages from the FPS and its southern extension, Likoudi/Drimos and Prosilio/Lava (4–6 in Fig. 1; Velitzelos et al., 2014). The focus of previous palaeobotanical studies in the FPS has been on macrofossils. In contrast, no comprehensive study of dispersed pollen and spores has been carried out in the FPS. While fruit and seed floras, to a great extent, and leaf floras, to a lesser extent, reflect local vegetation in an area, dispersed pollen and spores provide additional information about the regional vegetation. Therefore, a main focus of the present study is on spores and pollen of the Messinian plant assemblage of Vegora.

We (*i*) investigated dispersed spores and pollen using a combined light and scanning electron microscopy approach (Daghlian, 1982; Zetter, 1989; Halbritter et al., 2018) that allows a more accurate determination of pollen and hence higher taxonomic resolution. We (*ii*) then compiled a complete list of plant taxa recorded for the site of Vegora including fruits and seeds, foliage, and spores and pollen. Based on the ecological properties of their modern analogue taxa, we assigned the fossil-taxa to functional types (vegetation units) and inferred palaeoenvironments of the FPS during the Messinian. Using leaf physiognomic characteristics, we (*iii*) conducted a Climate Leaf Analysis Multivariate Program (CLAMP) analysis (Spicer, 2008; Yang et al., 2011) to infer several climate parameters for the late Miocene of the FPS. We also (*iv*) used a modified "Co-existence approach" (Mosbrugger & Utescher, 1997; Greenwood et al., 2005) based on climatic requirements of modern analogue plant taxa to infer two climate parameters and (*v*) a Köppen signature analysis (Denk et al., 2013; Bouchal et al., 2018) based on the Köppen-Geiger climate types in which modern analogue taxa of the fossil-taxa occur. Finally, we (*vi*) discuss how well the translation of fossil plant assemblages into functional types (vegetation units, biomes) works for reconstructing past environments at local and regional scales.

2. Material and Methods

2.1. Geological setting

The old open-pit lignite quarry of Vegora is located in western Macedonia, northwestern Greece, ca. 2 km E of the town of Amyntaio and is part of the Neogene Florina-Ptolemais-Servia intermontane basin (FPS) and its northern (Bitola Basin) and southern extensions (Likoudi Basin; Fig. 1). The NNW–SSE trending FPS is ca. 120 km long and presently at elevations between 400 and 700 m a.s.l. and is flanked by mountain ranges to the east and the west. Main ranges include Baba Planina (Pelister, 2,601 m), Verno (2,128 m), and Askio (2,111 m) to the west of the basin and Voras (2,528 m), Vermio (2,065 m), Olympus (2,917 m) to the east (Fig. 1). These ranges are mainly comprised of Mesozoic limestones, Upper Carboniferous granites and Paleozoic schists.

Continuous sedimentation since 8 Ma resulted in the accumulation of ca. 600 m of late Miocene to early Pleistocene lake sediments with intercalated lignites and alluvial deposits. The FPS Basin formed in the late Miocene as a result of NE–SW extension in the Pelagonian Zone, the westernmost zone of the Internal Hellenides (Brunn, 1956; Pavlides & Mountrakis,

1986, 1987). A subsequent Pleistocene episode of NW–SE extension caused the fragmentation of the basin into several sub-basins (Steenbrink et al., 2006).

Basin fills overlay unconformably Paleozoic and Mesozoic rocks. Alpine and pre-Alpine basement of the area consists of Pelagonian metamorphic rocks (gneisses, amphibolites, mica schists, meta-granites and Permian to Triassic meta-sediments) and crystalline limestone of Triassic–Jurassic age (carbonate cover). Subpelagonian ophiolites and deep-sea sediments of Jurassic age, comprising the Vourinos ophiolitic complex, thrust over the Pelagonian carbonate rocks and are covered by Cretaceous strata (Brunn, 1956; Mavridis et al., 1977; Pavlides & Mountrakis, 1986, 1987; Roberts et al., 1988).

The Vegora section belongs to the ca. 300 m thick Komnina Formation, which unconformably overlies pre-Neogene basement and is predominantly composed of alluvial sands and conglomerates, lacustrine (diatomaceous) marls and palustrine clays, with some intercalated (xylite-type) lignite seams (Steenbrink et al., 2006). The detailed description of the sequence at the Vegora quarry follows Kvaček et al. (2002) and Steenbrink et al. (2006) (Fig. 2). Since 2000, the lower part of the sequence was not accessible and the exposed sequence started with a ca. 10 m thick lignite seam (see fig. 3 in Kvaček et al., 2002 versus fig. 2, unit 1, in Steenbrink et al., 2006 corresponding to unit 1 in the present Fig. 2).

The full Vegora section begins with hard marls (>15 m) followed by 10–15 m of clay sands and a white marl layer of 10 m. Then, a formation of clay sands follows with a total thickness of 15–20 m. This formation starts with lignitic marls followed by marls and clay sand intercalations. The sand is rich in mica.

Above this, a lignite seam occurs with a thickness of 12–35 m. Within the seam, three xylitic layers with a total thickness of 10–12 m can be distinguished. The lower xylitic layer is about 3–4 m, the middle 0.5–1.5 m and the upper is 4–9 m in thickness (Kvaček et al., 2002).

The upper lignite layer was the first visible layer in 2002 in the section (unit 1 in Fig. 2). Between the xylitic layers, sand layers of various thickness (0 to 15 m) occur. In general, the thickness of these sand layers is smaller towards the N and NE ends of the mine and becomes significantly larger towards the W and SW ends of the mine.

The top of the upper xylitic layer is covered by 3–4 m thick shales, followed by a thick layer of light blue marls, 10–60 m thick (unit 2 in Fig. 2), and a layer of sandy marls, 10–40 m thick (units 3 and 4 in Fig. 2). Unit 3 is made up of grey-brown lignitic clay at its base and multi-coloured mottled clays, silts and fine sands higher up. Unit 4 consists of cross-bedded conglomerates and coarse sands at the base overlain by mottled clays, silts and fine sands with calcareous nodules. Finally, the top of the section is made up of dark red, mottled sands, silts and clays (unit 5).

Unit 2 of Steenbrink et al. (2006) corresponds to the main fossiliferous layers for plant fossils and diatoms (Gersonde & Velitzelos, 1978).

The uppermost layer of the Neogene sediments in the area is a formation of marly limestones, of different thickness, which is not everywhere visible appearing only at the nearby villages of Neapoli and Lakia. All Neogene sediments of the area are inclined by a 10º slope towards NNW.

The rocks on the top of the Neogene section are Quaternary alluvial deposits, conglomerates, sands, and gravels. This material, in general, has been supplied from erosion processes of the nearby metamorphic mountains.

2.2. Age

In the upper part of unit 2, 4 cm-thick layers of tephra rich in biotite were found and used for $^{40}Ar/^{39}Ar$ dating (Steenbrink et. al., 2006). The calculated age of 5.97 ± 0.07 Ma corresponds to pre-evaporitic Messinian and provides an independent age constraint for correlation with the Subchron C3An.1n. In addition, using palaeomagnetic data, the base of unit 2, just above the lignite seam, can be correlated to the astronomical polarity timescale, indicating that its position corresponds to the end of Subchron C3An.2n. This would suggest an age of ca. 6.4 Ma for the beginning of unit 2. Therefore, the period of deposition of the light blue marls (unit 2) from Vegora can be narrowed down to ca. 400 ka.

2.3. Sample processing

The palynological sample was taken from a slab piece (S115992) from a leaf layer in unit 2 of the Vegora mine. The sample was processed following standard protocols (20% HCl to dissolve carbonate, 40% HF to dissolve silica, 20% HCl to dissolve fluorspar; chlorination, acetolysis; see Halbritter et al., 2018) and the residue was transferred to glycerol.

2.4. Palynological investigation

Light microscopy (LM) micrographs were taken with an Olympus BX51 microscope (Swedish Museum of Natural History [NRM], Stockholm, Sweden) equipped with an Olympus DP71 camera. The same grains were examined using LM and scanning electron microscopy (SEM; single grain method; Zetter, 1989; Halbritter et al., 2018). Specimens were sputter-coated with gold for SEM investigation. SEM micrographs were taken with an ESEM FEI Quanta FEG 650 SEM (Stockholm University). Residue and SEM stubs are stored at NRM under specimen numbers S11599201–S11599220. Terminology of palynomorphs follows Punt et al. (2007) and Halbritter et al. (2018). Size categories follow Halbritter et al. (2018). Palynomorphs were determined to family, genus or infrageneric level. In cases when no taxonomic affinity could be established, we used fossil form taxa which are not implying a particular systematic affiliation. The systematic palaeobotany section starts with algae, fern and fern allies, gymnosperms and is followed by angiosperms. Angiosperm classification and author names of orders and families follow APG IV (2016).

2.5. Inferring palaeoclimate estimates

We employed three different (semi)quantitative methods to infer a range of climate parameters for the Messinian of NW Greece.

CLAMP (climate leaf analysis multivariate program) is a physiognomy based, taxon free method of climate inference and makes use of the relationship between leaf architecture and climate. CLAMP uses calibration datasets of modern vegetation sites across the world to place a fossil leaf assemblage in physiognomic space, which then can be translated into numeric values for several climate parameters (Spicer, 2008; Yang et al., 2011).

The Coexistence Approach (CA; Utescher et al., 2014) is a method of inferring palaeoclimate based on nearest living relatives (NLR) of fossil taxa. CA assumes that for a given climate parameter, the tolerances of all or nearly all taxa in a fossil assemblage will overlap to some degree; this overlap is called the climatic coexistence interval. In a slight modification of this approach (Greenwood et al., 2005) the zone of overlap was calculated using the 10th percentile (lower limit) and 90th percentile (upper limit) of the total range for all taxa recorded for a single flora. Following best practices in applying the CA Utescher et al. (2014) provided several guidelines to apply the CA in a meaningful way. Among these guidelines, one is to exclude relict taxa (usually monotypic or comprising very few extant species) from

the analysis, because of their likely unrepresentative modern distribution. Examples for such taxa are the East and Southeast Asian *Craigia* and *Glyptostrobus*. These taxa had a much wider distribution during parts of the Cenozoic including Arctic regions. For example, Budantsev & Golovneva (2009) described *Craigia* from the Eocene Renardodden Formation of Spitsbergen for which they inferred a mean annual temperature (MAT) of 8.4 °C and a coldest month mean temperature (CMMT) of –1 °C based on a CLAMP analysis. In contrast, the two modern species occur in climates with MAT 13.2–21 °C and CMMT 6.3–14.2 °C (Fang et al., 2009). Hence, it is assumed that for relict plants ecological niches may have changed considerably during the Cenozoic (e.g. Kvaček, 2007). For further assumptions of the CA and their critique, see Grimm & Potts (2016) and Grimm et al. (2016). Climate parameters for the NLR are given in the *electronic supplementary material Table S1*.
Köppen signatures (Denk et al., 2013; Bouchal et al., 2018) is another approach to infer large-scale climatic patterns for the Cenozoic that is based on NLR of fossil taxa. Modern distribution ranges are mapped on Köppen-Geiger climate maps (Kottek et al., 2006; Peel et al., 2007; Rubel et al, 2017; Global_1986-2010_KG_5m.kmz; see Table 1 for explanations of Köppen-Geiger categories) and the Köppen climate types in which the modern taxa occur are taken as a proxy for the climate space in which the fossil taxa occurred. It is explicitly stated that climate niche evolution will negatively impact the reliability of the inferred palaeoclimate. To overcome this drawback, subgenera, sections, and genera are used as NLR, whereas single species are usually not considered for NLR. The representation of different climate types is first scored for each species within a genus as present (1)/absent (0) (*electronic supplementary material Table S2*). To summarize preferences for climate types of all modern analogues, an implicit weighting scheme is used to discriminate between modern analogues that are highly climatically constrained and those that occur in many climate zones. For each modern species, the sum of its Köppen signature is always 1. For example, if a species is present in two Köppen–Geiger climate types, *Cfa* and *Cfb*, both score 0.5. If a species is present in 10 Köppen–Geiger climate types, each of these climate types scores 0.1. The Köppen signature of a genus or section, the preferred NLR of a fossil taxon, is the sum of its species' Köppen signatures for each climate type divided by the total number of scored species for this genus. By this, the percentage representation of each Köppen–Geiger climate type is determined for a genus/section (Bouchal et al., 2018). For pollen taxa of herbaceous and a few woody angiosperm groups that are resolved to family-level only, the distributions of extant members of the family were combined into a general family distribution range and the corresponding Köppen–Geiger climate types determined.

2.6. Characterisation of terrestrial biomes

For convenience, we use the biome classification of Woodward et al. (2004) that recognizes five major tree biomes based on the physiognomy of the dominant species: *Needleleaf evergreen* (NLE), *needleleaf deciduous* (NLD), *broadleaf evergreen* (BLE), *broadleaf cold deciduous* and *broadleaf drought deciduous* (BLD_{cold}, $BLD_{drought}$), and MIXED forests, which consist of tree communities with interspersed mixtures or mosaics of the other four tree biomes. These authors also observed that broadleaf drought deciduous vegetation grades substantially into broadleaf evergreen vegetation. Besides, *shrublands* are defined as lands with woody vegetation less than 2 m tall. *Savannahs* are defined as lands with herbaceous or other understorey systems, where woody savannahs have forest canopy cover between 30 to 60 %, and savannah has forest canopy cover between 10 and 30 % (Woodward et al., 2004). This very broad definition of savannah may be strongly oversimplified. Thus, for savannah-

like vegetation, we make a distinction between *steppe* and *forest-steppe* of temperate regions with a continuous layer of C_3 grasses and *savannah* and *woody savannah* of tropical regions with a continuous layer of C_4 grasses (Ratnam et al., 2011).

3. Results

3.1. Pollen and spores: diversity and environmental signal

We determined more than 50 palynomorph taxa from a leaf layer in unit 2 of the Vegora section (Figs 3–5). A comprehensive taxonomic account including pollen morphological descriptions and additional LM and SEM micrographs is provided in the *electronic supplementary material S3*. The fossil-taxa comprise two algae, five ferns, twelve herbaceous plants, one woody liana, and more than 30 woody trees and shrubs (Table 2). Besides the taxonomic evaluation, 430 palynomorphs were counted to assess the abundance of different taxonomic groups, life forms, and pollination syndromes (Table 3; Fig. 6). Roughly, half of the pollen taxa were present in very small amounts (1–3 grains in the counted sample or < 1%; *electronic supplementary material Table S4*). The presence and abundance of *Spirogyra* zygospores/aplanospores indicate a lake with shallow lake margins (reed belt with *Typha*) and stagnant, oxygen-rich, open freshwaters. Spores of *Osmunda* (> 4%) and *Leavigatosporites haardti* (> 1.6%) are of moderate abundance suggesting that the producing pteridophytes grew close to the sedimentation area, the Messinian Vegora Lake. Among conifers and wind-pollinated trees, strong pollen producers such as *Pinus* (subgenus *Strobus* 11%, subgenus *Pinus* ~8%), *Abies* (8.4%), *Cathaya* (7%), the Betulaceae *Alnus* (9.3%) and the Fagaceae *Fagus* (7%) are most abundant. Another group of wind-pollinated trees and shrubs was represented with abundances between 2% and 5%. Among these were both deciduous and evergreen oaks (*Quercus*) and conifers such as *Cedrus* and *Tsuga* and undifferentiated papillate Cupressaceae.

Among the taxa that are represented by single or few pollen grains, a significant number belonged to insect-pollinated plants. Insect-pollinated trees, shrubs and lianas include *Craigia*, *Platycarya*, Castaneoideae and *Parthenocissus*; *Hedera* and *Sassafras* are further insect-pollinated woody taxa, recorded in the leaf fossil record. Herbaceous taxa comprise Apiaceae, Caryophyllaceae, *Geranium*, *Succisa*, Asteraceae and Cichorioideae.

The ratio arboreal pollen (AP) to non-arboreal pollen (NAP) is 89.5% to 10.5% indicating a forest dominated (tree prevalent) local and regional vegetation according to the threshold values of Favre et al. (2008). Forest types (biomes of Woodward et al., 2004) represented by the pollen assemblage are needleleaf evergreen and deciduous forests (NLE, NLD), broadleaf deciduous forests (BLD), broadleaf evergreen forests (BLE) and mixed forests (MIXED). In addition, BLD and NLD either thrived on well-drained soils or in temporally or permanently inundated areas.

A few taxa might also indicate the presence of closed or open shrublands and grasslands (herbaceous taxa including sparse Poaceae with affinity to *Poa/Lolium*, Chenopodioideae, Apiaceae etc. and woody taxa including palms; see Table 2 for other woody taxa). These may have been associated with BLE woodlands (*Q. mediterranea*, *Q. sosnowskyi*) or with mesophytic evergreen forests of *Q. drymeja* (see below). Alternatively, they may have originated from an independent vegetation type (for example montane grasslands).

Among needleleaf forest biomes, for some taxa, the attribution to a distinct forest type is not straightforward. For example, conifers such as *Cathaya* may have been part of the montane hinterland vegetation on well-drained soils but may also have been important elements of peat-forming vegetation (Schneider, 1992; Dolezych & Schneider, 2006, 2007, 2012).

Based on pollen abundances (*electronic supplementary material Table S4*) local (close to the lake), regional (occurring in the FPS) and extra-regional (potentially occurring outside the FPS) vegetation can be inferred. Local vegetation consisted of BLD forests subjected to flooding (*Alnus*) and NLD swamp forests (papillate Cupressaceae; Bouchal & Denk, 2020). Close to the lake, a mixed forest with *Fagus*, *Abies* and *Cathaya* thrived (using the modern Abant Gölü of northern Turkey as a reference for pollen rain vegetation relationships; van Zeist & Bottema, 1991). Deciduous oaks (mainly of sect. *Cerris*) also might have been part of local forest vegetation (BLD). *Pinus* and *Cedrus* NLE forests and evergreen oak forests (BLE) grew at some distance from the lake (regional vegetation; using threshold abundances of *Cedrus*, 7%, and evergreen *Quercus*, 20%, as indicators of local source vegetation; Bell & Fletcher, 2016).

3.2. Fossil leaves, fruits, and seeds: diversity and environmental signal

Leaf and fruit remains from the Vegora mine have been collected and described since half a century (Schneider & Gregor, 1977, 1979; Velitzelos & Gregor, 1985, 1990; Knobloch & Velitzelos, 1987, Mai & Velitzelos, 1997). The most recent reviews are those of Kvaček et al. (2002) and Velitzelos et al. (2014). Table 2 provides an updated taxon list. Fruits and seeds recovered from the lignite seam of the Vegora section represent aquatic and reed vegetation. From the lignite seam also trunks of tall trees (as *Sequoioxylon*, Velitzelos et al., 2002) in upright position were recovered. The plant assemblage of the blue marls represents needleleaf evergreen and deciduous, and broadleaf evergreen and deciduous, as well as mixed forests. Among needleleaf forests, freshwater swamp forests are typically represented by Taxodioideae, while Sequoioideae, *Keteleeria*, *Pinus* and others may have grown on water-saturated peat and on well-drained soils of the hinterland (forest types NLE, NLD). Based on the great abundance of *Alnus* leaves, a local alder swamp may also be inferred (BLD). *Fagus* is among the most abundant taxa based on the number of recovered leaf remains suggesting that it was part of the mesic forest vegetation close to the lake. Also, deciduous foliage of *Quercus* sect. *Cerris* (*Q. kubinyi*, possibly *Q. gigas*) might have grown in the vicinity of the lake, either forming mixed stands with *Fagus* or oak-dominated forests. Kvaček et al. (2002) referred to this vegetation as *Fagetum gussonii*/*Quercetum mixtum*.

Evergreen oaks are abundant in the Vegora leaf assemblage but fairly rare in the pollen record (Table 3). This indicates that the leathery leaves of these taxa were transported to the area of sedimentation by slow-flowing streams and that the source vegetation was further away from the lake. Kvaček et al. (2002) referred to these evergreen forests as sclerophyllous (*Quercetum mediterraneum*). Denk et al. (2017b) distinguished between extant sclerophyllous Mediterranean oak forest and laurophyllous *Q. floribunda* forest from Afghanistan which is a better analogue for the widespread western Eurasian fossil-taxon *Q. drymeja*. Hence, we infer an ecological cline from mesic evergreen oak forests to sclerophyllous forest and shrublands in the Messinian of Vegora (cf. Freitag, 1971, 1982).

Well-drained forests dominated by needleleaf taxa occurred in the montane vegetation belt (*Abies*) and on rocky substrates (*Cedrus*, *Pinus*). Only a few taxa are potentially representing open shrubland vegetation (*Acer* spp., *Chamaerops*).

3.3. Inferring past climate with CLAMP

In this study, 41 dicot leaf morphotypes were scored for the CLAMP analysis. Given the distinctly temperate appearance of this flora, we used the calibration dataset *Physg3arcAZ_GRIDMet3arAZ*. *Physg3arcAZ* includes 173 sites, among them the 144

Physg3brcAZ sites plus 29 sites corresponding to the alpine nest (Wolfe, 1993). The alpine locations are the coldest sites known to have a different physiognomic behaviour (Wolfe, 1993); they are characterised by a WMMT lower than 16 °C and a CMMT lower than 3 °C (Wolfe, 1993). The reconstructed climate parameters are MAT 10–13.5 °C, WMMT 19.2–22.8 °C, CMMT 1–5 °C, GROWSEAS 6–8 months, GSP 700–1100 mm, MMGSP 110–160 mm, Three_WET 500–780 mm, Three_DRY 180–260 mm, and Three_WET to Three_DRY ratio < 4 (Table 4). In terms of the Köppen-Geiger climate classification, this translates into a temperate *Cfb* climate (T_{cold} > 0 and < 18 °C; without a dry season; warm summer T_{hot} < 22 °C).

In addition, we used the calibration dataset *PhysgAsia1_HiResGRIDMetAsia1* that adds 45 sites from China to the *Physg3brcAZ* dataset. Using this dataset, the reconstructed climate parameters are generally cooler and drier than the ones obtained from *Physg3arcAZ*. MAT 8.7–11.5 °C, WMMT 19–22.6 °C, CMMT -2.7–2.3 °C, GROWSEAS 5.5–7 months, GSP 460–1100 mm, MMGSP 100–160 mm, Three_WET 400–750 mm, Three_DRY 80–220 mm, and Three_WET to Three_DRY ratio < 5.5. In terms of the Köppen-Geiger climate classification, this translates into a temperate *Cfb* to cold *Dfb* climate (T_{cold} > 0 and < 18 °C versus T_{cold} < 0 °C; both without a dry season and warm summer T_{hot} < 22 °C). Score sheets and full documentation of the CLAMP analyses are provided in *electronic supplementary material S5*.

3.4. Inferring past climate with CA

Using the coexistence approach, we estimated coldest month mean temperature (CMMT) and mean annual temperature (MAT) coexistence intervals to see how CA behaves including and excluding relictual and monotypic taxa. Following Utescher et al. (2014) relict taxa with very limited modern distribution were excluded from the analysis. Excluded taxa are plotted to the left of the diagram in Fig. 7. For the monotypic genus *Chamaerops*, the tribus Trachycarpeae was used as NLR. For CMMT a lower boundary value of 1.2 °C is estimated based on the cold tolerance of Trachycarpeae. *Chamaerops* has a slightly warmer CMMT of 4 °C. For mean annual temperature (MAT) the lower boundary is defined by *Zelkova* (8.6 °C) and the upper boundary by *Acer* sect. *Acer* (21.2 °C). When only the 10–90% percentiles were considered, MAT low was defined by *Zelkova* as 9.9 °C and MAT high by *Acer* sect. *Acer* as 18.4 °C (Table 4; Fig. 7).

Inclusion of *a priori* excluded relict species with a limited distribution would greatly change the estimated climate values. CMMT low would be defined by *Craigia* (6.5 °C) and CMMT high by *Sequoia* (7.5 °C). Likewise, MAT low would be defined by the monotypic conifer *Cathaya* (13.4 °C) and MAT high again by *Sequoia* (15.3 °C; *electronic supplementary material Table S1*).

Using only the 10–90% percentiles, MAT low would be defined by *Craigia* (14 °C) and MAT high (14.1 °C) by *Sequoia*.

3.5. Inferring past climate with Köppen signatures

Based on 700 Köppen signatures of modern species (rarely sections and families) genus- to family-specific Köppen signatures were used to generate Köppen signatures for the Vegora assemblage of unit 2. Temperate *C* climates are by far the most common ones represented by modern analogues of the Vegora plant assemblage. *Cfa/b* and *Cwa/b* climates represent 50% of the occurrences of NLR taxa when pollen and spores are considered, and 54% when macrofossils are considered (Fig. 8). *Csa/b* climates are represented by 11–13%. Snow

climates (CMMT < 0°C) are represented by 17% (*Df*, *Dw*) and 2–3% (*Ds*). Thus, *C* and *D* climates make up > 80% of all NLR occurrences. In contrast, equatorial climates are represented by 10% (spores and pollen) and 6.5% (macrofossils). Arid *B* climates are represented by < 10% in the spores/pollen and macrofossil assemblages.

4. Discussion

4.1. How well do plant fossils reflect past environments of the FPS?

It has long been known that there is no exact relationship between fossil (and modern) assemblages of dispersed spores and pollen and the actual vegetation (e.g. van Zeist et al., 1975; Connor et al., 2004; Traverse, 2007; Bell & Fletcher, 2016; Marinova et al., 2018). Marinova et al. (2018) pointed out several problems when inferring vegetation from pollen diagrams. These included (*i*) pollen production biases which generally result in the over-representation of woody species and the under-representation of herbaceous species in the pollen assemblage, (*ii*) transport of tree pollen into non-forested areas resulting in poor delineation of ecotonal boundaries, (*iii*) upslope transport of pollen from lowland areas in upland areas resulting in poor delineation of altitudinal vegetation gradients and tree line. Furthermore, these authors found that samples from small basins (<1 km^2) are more likely to be reconstructed accurately because they sample an appropriate pollen source area to reflect regional vegetation patterns in relatively heterogeneous landscapes. In contrast, large uncertainties were observed when inferring the local vegetation in large basins, e.g. the Black Sea. Here, large pollen source areas result in strongly mixed signals which do not well discriminate the vegetation belts around a specific site.

We note that this caveat may, in fact, be beneficial when inferring the past vegetation in a larger area. The FPS is a basin that extends ca. 120 km x 30 km and is flanked by high mountains. Hence, a rich pollen assemblage with a strongly mixed signal is expected to reflect the actual vegetation types in the region although it may be challenging to correctly assign particular pollen types to vegetation units. For instance, Ivanov (2001) interpreted a pollen diagram from a Tortonian section in the Sandanski Graben (Bulgaria; 8 in Fig. 1) with a considerable amount of herbaceous pollen (including Poaceae, Amaranthaceae/Chenopodioideae, and *Artemisia* making up c. 5 to 20% of the pollen spectrum) to reflect extra-regional open vegetation on an elevated plateau in addition to swamp forests, riparian forests, and mixed mesophytic forests developed in a river valley and adjoined slopes. Here, downslope transportation of pollen from open landscapes blurred the local signal of the pollen record, but at the same time added regional and extra-regional vegetation information.

A close relationship between the actual vegetation and the pollen spectrum from recent and Holocene sediment samples has also been reported for northwestern Turkey (van Zeist & Bottema, 1991). Modern surface-sample spectra accurately depicted the regional vegetation, although some taxa were underrepresented in the pollen spectra while others were overrepresented. For example, pollen spectra of *Fagus-Abies* dominated areas showed relatively low percentages of these two taxa (10.4% and 7.4%), while high amounts of *Pinus* (ca. 30%) derived from forests thriving at some distance from the pollen trap. Likewise, comparatively high amounts of *Juniperus*, *Quercus*, and *Carpinus* did not reflect the local vegetation but a regional signal. In combination with a weak herbaceous signal (Poaceae < 5%; Amaranthaceae/Chenopodioideae, Caryophyllaceae, Apiaceae represented by single pollen grains) the strong arboreal signal provided a fairly accurate picture of the forest communities at a regional scale (van Zeist & Bottema, 1991). In cases of bad pollen

preservation (oxidised sedimentary rocks) it should be kept in mind that only pollen with durable exines (high sporopollenin content) will be preserved (e.g. *Pinus*, Amaranthaceae/Chenopodioideae; Traverse, 2007) resulting in a biased signal.

In contrast to dispersed spores and pollen, macrofossils (leaves) mainly reflect local and regional vegetation whereas extra-regional vegetation is usually not reflected. Leaf remains are mostly scattered isolated carbonised compression fossils, which are not concentrated abundantly ("Blätterton" layers or paper shales) in distinct fossiliferous layers (Kvaček et al., 2002); both small and larger leaves are usually not fragmented and hence there is no indication for long-distance transport in high-energy depositional settings. At the same time, low pollen abundances of evergreen oaks along with abundant leaf fossils representing evergreen oaks might indicate that these leaves were transported by slow-flowing streams over relatively large distances. Rarely, large fruit bodies are encountered, mostly represented by conifer cones. Therefore, a combined wind and water transport from habitats bordering the lake can be assumed (Kvaček et al., 2002). Among woody plants, Fagaceae (*Fagus*, *Quercus*) are ecologically diverse and niche conserved at the genus/section level. *Fagus* is exclusively found on well-drained soils and hence was not an element of the swamp forest vegetation. However, under humid equable climates, lowland coastal and deltaic forests may contain *Fagus* and hardwood hammocks with rich broadleaf deciduous and evergreen forests may be present next to aquatic and hydric vegetation (Ferguson et al., 1999). In contrast, white oaks, sect. *Quercus*, may thrive in swamp forests, riparian forests, mesic forests of lowlands and uplands, or may form Mediterranean scrub. These different ecologies are well reflected in leaf morphology whereas pollen morphology at the sectional level does not discriminate different species/ecologies (Denk & Grimm, 2009). Since white oaks are represented by pollen only, no further conclusions can be drawn as to their ecologies. Other sections of *Quercus* (sects *Cerris*, *Ilex*) represented in the Vegora assemblage are highly niche conserved and exclusively found on well-drained soils. Based on differences in leaf morphology (leaf size, deciduousness), fossil-taxa such as *Quercus gigas* (leaf lamina up to 22 cm long; sect. *Cerris*) might indicate humid temperate conditions on northern slopes (Kvaček et al., 2002), while *Quercus kubinyi* (*Cerris*) might have been part of drier slopes. These fossil-species could have been accessory elements in *Fagus*-dominated or oak-dominated forests (see above, *Results* section). Section *Ilex* comprises evergreen species exclusively growing on well-drained soils. Closest relatives of the Messinian taxa are modern Mediterranean species (the fossil-species *Q. sosnowskyi* resembles the modern species *Q. alnifolia*, endemic to Cyprus, by leaf shape and leaf epidermal features; Kvaček et al., 2002) and Himalayan/East Asian species (e.g. *Q. drymeja* resembles the modern *Q. floribunda*, south of the Himalayas; Denk et al., 2017). Inferring the ecological properties of these fossil-taxa is not straight-forward: Morphologically they either resemble modern East Mediterranean taxa or temperate Himalayan taxa. At the same time, time-calibrated molecular phylogenies suggest that the modern Mediterranean members of sect. *Ilex* diverged from their Himalayan sister species during late Oligocene to early Miocene times, long before the deposition of the plant assemblage of Vegora (Jiang et al., 2019). Within the Mediterranean clade, the most mesic species *Q. ilex* also occurs in humid temperate forests of the Euxinian region (northern Turkey, western Georgia) and diverged from the remaining species of western Eurasian sect. *Ilex* no later than 9 Ma (Jiang et al., 2019). Assuming that fully Mediterranean climate conditions, with precipitation minima during the summer, in the Mediterranean region did not establish prior to the early Pliocene (Suc, 1984; Velitzelos et al., 2014) we speculate that the Messinian members of sect. *Ilex* were chiefly temperate species that went extinct during the

Pliocene (cf. Jiang et al., 2019). Specifically, *Q. drymeja* might have formed a forest belt above the *Fagetum gussonii*/*Quercetum mixtum* and below the needleleaf evergreen forest belt. Other *Quercus* sect. *Ilex* such as *Q. mediterranea* and *Q. sosnowskyi* may have formed woody shrublands or forests on drier sites (edaphically or due to the aspect of the slope). Concerning the presence of grasslands or open woodlands, the palaeobotanical data at hand cannot discriminate between different scenarios. For taxa that are known from the macrofossil record (*Chamaerops*, evergreen oaks) it is almost certain that they were part of the regional flora of the FPS. The woody genera *Olea*, *Cotinus*, and *Pistacia*, known only from the pollen record of unit 2, are typical elements of the present Mediterranean and submediterranean vegetation belt in Southern Europe. Bell & Fletcher (2016) found that soil samples in open vegetation plots in Northern Morocco recorded 20% to 35% arboreal pollen (AP). Main contributors to this regional to extra-regional airborne pollen rain were *Quercus* types and *Olea*. In our sample, arboreal pollen makes up almost 90% of the total count. *Quercus* certainly was a major component of local to regional vegetation because it is the most prominent component with several deciduous and evergreen species in the leaf flora of Vegora. In contrast, *Olea* makes up less than 1% in the pollen count. No leaf and seed remains reminiscent of *Olea* are recorded from Vegora. This along with the known ability for long-distance transport (Bell & Fletcher, 2016) might indicate the presence of *Olea* at a greater distance from the Vegora Basin. The same can be assumed for *Cotinus* and *Pistacia*. The latter, however, do also occur in open-canopy pine forests.

In case of herbaceous taxa represented by single or very few pollen grains in the palynological record, these may also reflect long-distance dispersal from high mountain or even from more distant coastal areas to the west of the FPS. They would then provide an extra-regional vegetation signal. Potential elements of open vegetation include Apiaceae, Amaranthaceae/Chenopodioideae, Poaceae, *Geranium*, Caryophyllaceae, Asteraceae and Cichorioideae. Except for Poaceae and Amaranthaceae/Chenopodioideae, these taxa are predominantly insect-pollinated. For wind-pollinated taxa represented with 1–3 grains in the pollen count (Poaceae, Amaranthaceae/Chenopodioideae) we assume that this is indicative of a regional or extra-regional source vegetation. The insect-pollinated taxa, also represented by 1–3 grains in the pollen count, are difficult to assign to either local or regional/extra-regional vegetation. If these groups were local elements, they would have been quite rare, based on the low numbers of their pollen grains. They could have been part of the lakeshore vegetation, of open rocky places, of the understorey of forest vegetation or meadows above the tree line. Alternatively, these elements could have been brought in by long-distance dispersal (LDD) from coastal plains to the southeast and east of the FPS.

In sum, the combined macrofossil and microfossil record offers an accurate picture of the different vegetation types present in the FPS during the Messinian. The fossil record suggests that the local and regional vegetation in the FPS comprised a range of ecologically different zonal and azonal forest types, while LDD of several herbaceous taxa may potentially have contributed to an extra-regional pollen signal.

4.2. Inferring Messinian pre-evaporitic vegetation of the FPS and adjacent areas

Our multi-proxy palaeobotanical study of the Messinian assemblage of Vegora is based on information from fruits and seeds, leaves, and dispersed pollen and spores. For the main flora in unit 2 (blue marls) we used information from leaf fossils and dispersed spores and pollen. As discussed above, there is strong evidence for the presence of a wide range of forest and forest/shrubland types in the FPS. Furthermore, a small number of woody and herbaceous

taxa could reflect open vegetation. The latter are represented by low numbers of pollen grains, which could be ascribed to LDD from remote areas including dry uplands or coastal plains. In order to evaluate the pre-evaporitic Messinian vegetation of the FPS, we compared our finds with previously published data on other plant fossil localities in the FPS and surrounding areas. In addition, a vertebrate locality from the Axios valley (Dytiko1, 2, 3; 3 in Fig. 1) is roughly coeval with the Messinian pre-evaporitic assemblages of the FPS (Koufos, 2006). The hypsodonty index of this fauna of 1.45–1.86 (The NOW community, 2020) corresponds to the diet types “mixed-closed habitats”, “regular browsers”, and “selective browsers” according to Janis (1986) and hence provides an excellent match with the environments inferred for the FPS.

From Lava (Fig. 1), Steenbrink et al. (2000) investigated two sequences covering two sedimentary cycles each. Based on palaeomagnetic correlation these sequences are dated as c. 6.8–6.7 Ma and c. 6.3 Ma. The pollen assemblages are comparable to the Vegora assemblage but differ in some respects. First, the Lava sections have a continuous high amount of *Pinus* pollen (20 to >60%) suggesting that the fossil site was located closer to pine forests than was the Vegora lake. Second, *Cedrus* pollen is abundant with values between 10 and >30%. Third, Steenbrink et al. (2000) did not report evergreen oak pollen, although evergreen *Quercus* is known from Lava based on leaf fossils (Velitzelos et al., 2014). Steenbrink et al. (2000) inferred a humid temperate climate without dry season for the investigated sedimentary cycles. In addition, they suggested that expansions of *Fagus* accompanied by a decrease of *Abies* might reflect subtle increases in montane humidity. Overall, they suggested continuously wet and warm-temperate climate conditions for the investigated period for Lava.

Velitzelos et al. (2014) provided revised taxon lists for the roughly coeval macrofossil (leaves and fruits/seeds) localities Prosilio and Lava (age based on palaeomagnetic correlation, 6.7–6.4 Ma; Steenbrink et al., 2006). The macroflora is very similar to the one from Vegora in terms of composition. However, whereas *Quercus sosnowskyi* is among the most abundant elements in Vegora, only a few leaves represent this species in Prosilio; also *Glyptostrobus* is much less abundant. *Pinus* is represented by cones, leaf fascicles, and leafy branches; this is in accordance with the high amount of pine pollen documented in the palynological record. *Fagus* is a frequent element as well, while *Abies* is not recorded in the macroflora of Prosilio and Lava. From the Prosilio section, no comprehensive palynological study is available. However, Biltekin (2010) investigated a 5 cm thick green clay bed dated at 6.6–6.55 Ma (key bed II of Steenbrink, 2000) that represents an insolation minimum. This bed, void of leaf fossils, was identified from the Lava and Prosilio sections (Steenbrink, 2000) and is situated between the two palynological sections studied from Lava. The three samples from Prosilio investigated by Biltekin (2010) are similar to the Lava pollen assemblages (dominance of conifer pollen, low percentages of herbaceous pollen). However, the samples from Prosilio show peaks of *Pinus* and *Tsuga* (samples 1 and 3) and of Cupressaceae (sample 2) that are not known from other pollen assemblages in the FPS. In addition, sample 2 has moderate amounts of *Artemisia*. The deviating pollen spectrum from this layer was explained by uplifting of the surrounding region (Biltekin, 2010). Alternatively, the cooler appearance of this assemblage could reflect the insolation minimum recorded for this interval (Steenbrink, 2000).

Likoudi, 20 km S of Lava, is located in a small basin south of the main FPS (Fig. 1). The macroflora (leaves, fruits and seeds) is very rich (see revised and updated floral list in Velitzelos et al., 2014). The precise age of the Messinian diatomaceous marls is not clear (Knobloch & Velitzelos, 1986) although it clearly is pre-evaporitic. The flora is characterised by the high diversity of conifers (11 genera of Cupressaceae, Pinaceae, and Taxaceae

including *Torreya* – as *Egeria* sp. in Velitzelos et al., 2014). As in Vegora, *Fagus* is a dominating element. Other taxa (*Cercis*, *Laria*, cf. *Nerium*) are not known from other FPS floras. Well-preserved cones of *Cedrus* and cones and leafy twigs of *Cathaya* and *Taiwania* suggest that these genera were not growing at high elevations but nearby the area of deposition (lake). If coeval with the Lava deposits, this would explain the relatively high amounts of *Cedrus* pollen in the palynological section of Lava.

Ivanov & Slavomirova (2002) investigated a 70 m succession of lacustrine sediments in the Bitola Basin (Northern Macedonia; borehole V-466; 1 in Fig. 1) about 10 km E of Bitola and 40 km NNW of Vegora. Based on a vertebrate fauna on top of these sediments, the plant-bearing sediments are assigned a late Miocene age (Dumurdžanov et al., 2002; Ognjanova-Rumenova, 2005). From these sediments, abundant leaves of *Quercus sosnowskyi* have been reported (Dumurdžanov et al., 2002). The pollen assemblage is similar to the one from Vegora by its high amounts of woody taxa (both conifers and angiosperms) and the composition and very low abundance of herbaceous taxa. In contrast to the Vegora assemblage, few taxa are represented by high percentages (*Pinus* 20–40%, *Fagus* up to 10%, *Quercus* 10–20%, Taxodioideae and Sequoioideae 10–15%, and *Alnus*, up to 20%). In the Vegora sample, only *Pinus* reached more than 10% in the pollen count.

For North and Central Italy, Kovar-Eder et al. (2006) and Bertini & Martinetto (2008) reported prevalence of deciduous *Fagus* and *Quercus* in the northern parts whereas in addition sclerophyllous plants (e.g. *Quercus mediterranea*) were common in Messinian pre-evaporitic assemblages of Central and Southern Italy (Gabbro I, Senigallia, Palena).

From the Serres Basin (7 in Fig. 1), Psilovikos & Karistineos (1986), Karistineos & Ioakim (1989) and Suc et al. (2015) reported pollen assemblages that reflect lowland swamp forests (NLD and BLD) and hinterland vegetation including broadleaf deciduous and needleleaf evergreen forests. The age of these localities is younger than Vegora and based on mammal data (Koufos, 2006) and geological data (Suc et al., 2015) might have been deposited during the post-evaporitic Messinian or the earliest Zanclean.

It is remarkable that post-evaporitic and evaporitic Messinian floras from Italy (Bertini & Martinetto, 2008) and Greece (Velitzelos et al., 2014) mainly reflect moist conditions and persistence of forested environments. This is in strong contrast to conditions from Turkey, where steppe and steppe forest were established by the end of the middle Miocene (Denk et al., 2018). Hence, pre-evaporitic sedimentary rocks from the Dardanelles strait contain palynological assemblages that clearly demonstrate the presence of herb dominated coastal vegetation before the peak of the Messinian Salinity Crisis (Melinte-Dobrescu et al., 2009). In contrast, pre-evaporitic palynological assemblages from northwestern Bulgaria (Drenovets) and from the western Black Sea (site 380-A) show that herbaceous and steppe elements were nearly absent from this region (Fauquette et al., 2006; Jimenez-Moreno et al., 2007; Popescu et al., 2010). Fauquette et al. (2006) reconstructed palaeoclimate using the so called Climatic Amplitude Method, which takes into consideration requirements of modern analogue taxa and pollen abundances of individual taxa. These authors inferred a MAT of (10–) 15–20ºC, a CMMT > 5ºC, and MAP of 1000–1500 mm for the pre-evaporitic Messinian of site 380-A. This is slightly warmer than reconstructed palaeoclimate parameters for the Vegora assemblage (cf. Table 4).

Main vegetation types recognised for the pre-evaporitic Messinian of the FPS and their modern analogues are summarised in Table 5.

4.3. Inferring Messinian pre-evaporitic climate of the FPS and adjacent areas

Fruit/seed and leaf records mainly represent azonal vegetation and may not adequately reflect the zonal vegetation growing at some distance from the area of sedimentation. Zonal vegetation is mainly controlled by large-scale climate (regional, extra-regional). Azonal vegetation is controlled by edaphic conditions rather than large-scale climate. For these reasons, seed/fruit and leaf assemblages either used for physiognomic (CLAMP) or taxonomic (Köppen signatures, CA) methods may not be suitable for a meaningful (representative) climate reconstruction or they may reconstruct a local climate. However, as shown by Ferguson et al. (1999), under mild and humid climate conditions, the vegetation close to the area of sedimentation consists of a mosaic of vegetation types, some of which are composed of woody plants that also dominate the hinterland vegetation. For example, natural levee and hardwood hammock vegetation associated with azonal swamp, riparian and bog vegetation in southeastern North America contains taxa such as *Fagus*, *Magnolia*, *Ilex* spp., *Carpinus*, and *Symplocos*. In this case, the limitations outlined above are not valid. In drier, strongly seasonal climate settings, the azonal vegetation will not be sufficient to produce meaningful (representative) regional climate estimates.

When the palynological record is taken into consideration, both the local and the regional (hinterland, vertical vegetation belts) vegetation is likely to be captured. This is reflected in the much greater diversity of conifers and herbaceous taxa in the pollen record as compared to the macrofossil record in the Vegora assemblage. In addition, long-distance dispersal may add information from the extra-regional vegetation (e.g. *Olea*; van Zeist & Bottema, 1991; Bell & Fletcher, 2016).

The resulting differences in reconstructed climate/vegetation are seen in the Köppen signatures for the leaf fossil and pollen/spore records of Vegora (Fig. 8). Taxa extending into tropical climates are much better represented in the pollen record than in the leaf record. Therefore, Köppen signatures, although not providing exact values for different climate parameters, offer important qualitative information. This can be illustrated by comparing three floras from the East Mediterranean region, all dominated by *Quercus* spp. and *Fagus* and ranging in age from early Burdigalian to Messinian: The early Burdigalian flora of Güvem, Anatolia (MN3, 20–18 Ma; Denk et al., 2017, 2019) has a tropical signal of 16% in Köppen signatures from pollen and spore assemblages, whereas tropical signal from leaf fossils is 11.9%. The middle Miocene floras of the Yatağan Basin (Langhian/Serravallian, MN6/MN7+8; 14.8–13.8 Ma; Bouchal et al., 2018) show a trend from the more humid MN6 zone to the more arid MN7+8 zone with tropical signal from pollen and spore assemblages decreasing from 11% in pollen zones 1 and 2 to 7% in the transitional pollen zone 2/3. The tropical signal in Köppen signatures from the macrofossil assemblage from pollen zone 2 is 9%. In the pre-evaporitic assemblages of Vegora, the tropical signal is 9% and 6% for the pollen/spore and leaf assemblages.

In contrast, the coexistence approach (CA), in producing exact values for selected climate parameters, will be prone to produce hybrid climates if fossil assemblages represent a range of lowland azonal and hinterland vegetation and vegetation from different vertical belts. Such artificial climates may be randomly expressed as narrow coexistence intervals including different vertical vegetation belts, or in very broad coexistence intervals (cf. Table 4). Thus, Köppen signatures are considered a more dynamic way of climate reconstruction as they account for the possibility that different elements may derive from different vertical vegetation belts.

CLAMP (Physg3arcAZ) reconstructed WMMT, which corresponds with a temperate climate with warm summers, *Cfb* Köppen climate type, underscoring the temperate character of the

Vegora assemblage. The calibration set Asia 1 reconstructed a cooler climate with CMMT below 0°C. This would appear to be in conflict with the cold tolerance of the palm *Chamaerops* (cf. Fig. 7) that is recorded from the leaf record and palms in general as documented in the pollen record. However, all three approaches to reconstruct the pre-evaporitic Messinian climate of the FPS suggest a temperate climate with weak seasonality (Table 4).

In view of the relatively homogeneous vegetation signal from the FPS (both from dispersed spores/pollen and leaves), the inferred climate is highly plausible.

5. Conclusion

The present study used palaeobotanical data to reconstruct palaeoenvironments in an intermontane basin of northwestern Greece shortly before the Messinian salinity crisis. For the period 6.4–6 Ma, leaf fossil data and dispersed spores and pollen indicate the presence of various types of forest including riparian and mesic forests, deciduous and evergreen forests, laurophyllous forests and sclerophyllous woodlands. Open landscapes dominated by herbaceous plants were not reconstructed for the Florina-Ptolemais-Servia Basin. Based on sparse pollen records resulting from potential long-distance dispersal it cannot be ruled out that herbaceous plants played a more important role in coastal lowlands to the west of the study area. However, contemporaneous vertebrate faunas from the Axios valley also suggest mixed forested vegetation. We found that the combined leaf and dispersed spore/pollen records allow fairly accurate reconstruction of local and regional vegetation. Leaf fossils offer more species-diagnostic features than pollen and a combination of leaf taphonomy and pollen frequencies allow discriminating local and regional vegetation. Furthermore, specific comparison with modern pollen spectra was made in order to understand biases in pollen abundances. This provided a transfer function for the interpretation of fossil pollen assemblages. The results of this study confirm previous findings of a North to South gradient of temperature and precipitation seasonality in the Mediterranean area during the Messinian. Our results also reinforce the notion that steppe and forest-steppe environments evolved earlier in Turkey with deciduous oaks playing important roles in the woody flora. In contrast, laurophyllous evergreen oak forest persisted in Greece/Italy into the late Miocene and as relict into the Pliocene. Climate reconstructions utilizing three different approaches to climate reconstruction resulted in roughly similar values that translate into a cool temperate *Cfb* climate according to the Köppen-Geiger climate classification. When comparing CLAMP, CA, and Köppen signatures, we noticed that leaf assemblages may be biased towards autochthonous plant communities and by this, the climate signal will be highly local. However, under humid mild climates plants from the hinterland vegetation may thrive from lowlands to high altitudes and interspersed in riparian landscapes (e.g. on hammocks, gallery forests etc.). Furthermore, the taphonomy of the fossil plant assemblage of Vegora suggests that slow-flowing streams had transported leaves from different vegetation types of the hinterland into the lake and thus the leaf taphocoenoses would be representative of both the local and regional vegetation. This causes a further problem for CLAMP and more so for CA: climate signals in the fossil plant assemblage may be highly mixed and may derive from different vertical vegetation belts. Köppen signatures, while not generating exact values for particular climate parameters, overcome the problem of hybrid climates as they collect climatic/environmental signal in a plant assemblage without averaging different signals into a single, possibly artificial, signal.

Data accessibility. This article and all data used in this article are made available in bioRxiv. https://www.biorxiv.org/content/10.1101/848747v1
Supplementary Materials are available within the figshare repository:
https://doi.org/10.6084/m9.figshare.10327646.v1

Author's contributions. T.D. designed the study and wrote the first draft. J.M.B. investigated dispersed pollen and spores and made the Köppen signatures and CA analyses. T.H.G. made the CLAMP analysis. T.D., J.M.B., T.H.G., D.V., and E.V. evaluated the fossil data and wrote the final paper.

Competing interests. We declare we have no competing interests.

Funding. This study was financed by a grant of the Swedish Research Council (VR; project no. 2015-03986) to T.D. T.H.G. was supported by The Scientific and Technological Research Council of Turkey (TÜBİTAK), 2219 Post-Doctoral Research Fellowship Program (2017/2), project no. 1059B191700382.

Acknowledgements. We thank the associate editor Emily Lindsey. Valuable suggestions by the reviewers Jean-Pierre Suc and Jakub Sakala helped to improve the final manuscript.

References

Akhani H, Djamali M, Ghorbanalizadeh A, Ramezani E. 2010 Plant biodiversity of Hyrcanian relict forests, N Iran: an overview of the flora, vegetation, palaeoecology and conservation. Pak. J. Bot. **42**, 231–258.

Akkemik Ü. 2003 Tree rings of *Cedrus libani* at the northern boundary of its natural distribution. IAWA J. **24**, 63–73.

Angiosperm Phylogeny Group (APG). 2016 An updated of the angiosperm phylogeny group classification for the orders and families of flowering plants APG IV. Bot. J. Linn. Soc. **181**, 1–20.

Bell BA, Fletcher WJ. 2016 Modern surface pollen assemblages from the Middle and High Atlas, Morocco: insights into pollen representation and transport. Grana **55**, 286–301.

Bertini A, Martinetto E. 2008 Messinian to Zanclean vegetation and climate of Northern and Central Italy. Boll. Soc. Paleontol. Ital. **47**, 105–121.

Biltekin D. 2010 Végétation et climat des régions nord-anatolienne et nord-égéenne depuis 7 Ma d'aprés l'analyse pollinique. PhD thesis. Earth Sciences. Université Claude Bernard - Lyon I; Université Technique d'Istanbul.

Brunn JH. 1956 Contribution à l'étude géologique du Pinde septentrional et d'une partie de la Macédonie. Ann. Géol. Pays Hellèn. **7**, 1–358.

Bouchal JM, Denk T. 2020 Low taxonomic resolution of papillate Cupressaceae pollen (former Taxodiaceae) impairs their applicability for palaeo-habitat reconstruction. Grana **59**, 71–93.

Bouchal JM, Güner TH, Denk T. 2018 Middle Miocene climate of southwestern Anatolia from multiple botanical proxies. Clim. Past **12**, 1427–1440.

Budantsev LY, Golovneva LB. 2009 Fossil Flora of Arctic II - Palaeogene Flora of Spitsbergen. St. Petersburg: Komarov Bot. Inst. Russ. Acad. Sci.

Cerling TE, Harris JM, MacFadden BJ, Leakey MG, Quade J, Eisenmann V, Ehleringer JR. 1997 Global change through the Miocene/Pliocene boundary. Nature **389**, 153–158.

Connor SE, Thomas I, Kvavadze EV, Arabuli GJ, Avakov GS, Antonio Sagona A. 2004 A survey of modern pollen and vegetation along an altitudinal transect in southern Georgia, Caucasus region. Rev. Palaeobot. Palyn. **129**, 229–250.

Daghlian CP. 1982 A simple method for combined light, scanning and transmission electron microscope observation of single pollen grains from dispersed pollen samples. Pollen et Spores **24**, 537–545.

Denk T, Grimm GW. 2009 Significance of pollen characteristics for infrageneric classification and phylogeny in *Quercus* (Fagaceae). Int. J. Plant Sci. **170**, 926–940.

Denk T, Velitzelos D. 2002 First evidence of epidermal structure of *Ginkgo* from the Mediterranean Tertiary. Rev. Palaeobot. Palynol. **120**, 1–15.

Denk T, Frotzler N, Davitashvili N. 2001 Vegetational patterns and distribution of relict taxa in humid temperate forests and wetlands of Georgia (Transcaucasia). Biol. J. Linn. Soc. **72**, 287–332.

Denk T, Grimm GW, Grímsson F, Zetter R. 2013 Evidence from "Köppen signatures" of fossil plant assemblages for effective heat transport of Gulf Stream to subarctic North Atlantic during Miocene cooling, Biogeosci. **10**, 7927–7942. https://doi.org/10.5194/bg-10-7927-2013.

Denk T, Güner TH, Kvaček Z, Bouchal JM. 2017a The early Miocene flora of Güvem (Central Anatolia, Turkey): a window into early Neogene vegetation and environments in the Eastern Mediterranean. Acta Palaeobot. **57**, 237–338.

Denk T, Velitzelos E, Güner HT, Bouchal JM, Grímsson F, Grimm GW. 2017b Taxonomy and palaeoecology of two widespread western Eurasian Neogene sclerophyllous oak species: *Quercus drymeja* Unger and *Q. mediterranea* Unger. Rev. Palaeobot. Palynol. **241**, 98–128.

Denk T, Zohner CM, Grimm GW, Renner SS. 2018 Plant fossils reveal major biomes occupied by the late Miocene Old-World Pikermian fauna. Nature Ecol. Evol. **2**, 1864–1870.

Denk T, Güner HT, Bouchal JM. 2019 Early Miocene climate and biomes of Turkey: Evidence from leaf fossils, dispersed pollen, and petrified wood. Palaeogeogr., Palaeoecol., Palaeoclimatol. **530**, 236–248.

Dolezych M, Schneider W. 2006 Inkohlte Hölzer und Cuticulae dispersae aus dem 2. Miozänen Flözhorizont im Tagebau Welzow (Lausitz) – Taxonomie und vergleichende feinstratigraphisch-fazielle Zuordnung. Z. geol. Wiss. **34**, 165–259.

Dolezych M, Schneider W. 2007 Taxonomie und Taphonomie von Koniferenhölzern und Cuticulae dispersae im 2. Lausitzer Flözhorizont (Miozän) des Senftenberger Reviers. Palaeontograph. B **276**, 1–95.

Dolezych M, Schneider W. 2012 Fossil conifers in peat bog environments – results from the Central European Neogene. Japan. J. Palynol. **58** (Special Issue), 48.

Dumurdžanov N, Krstić N, Mihajlović D, Ognjanovo-Rumenova N, Petrov G. 2002 New data on stratigraphy of the Neogene and Pleistocene in Mariovo, Macedonia. Geol. Macedon. **17**, 43–52.

Erdős L, Ambarli D, Anenkhonov OA, Bátori Z, CserhalmiD, Kiss M, Kröel-Dulay G, Liu H, Magnes M, Molnár Z, et al. 2018 The edge of two worlds: A new synthesis on Eurasian forest-steppes. Appl. Vegetation Sci. **21**, 345–362.

Favre E, Escarguel G, Suc J-P, Vidal G, Thévenod L. 2008 A contribution to deciphering the meaning of AP/NAP with respect to vegetation cover. Rev. Palaeobot. Palynol. **148**, 13–35.

Fang J, Wang Z, Tang Z. 2009 Atlas of Woody Plants in China. Volumes 1 to 3 and index. Beijing: Higher Education Press.

Fauquette S, Suc J-P, Bertini A, Popescu S-M, Warny S, Bachiri Taoufiq N, Perez Villa, M-J, Chikhi H, Subally D, Feddi N, Clauzon G, Ferrier J. 2006 How much did climate force the Messinian salinity crisis? Quantified climatic conditions from pollen records in the Mediterranean region. Palaeogeogr., Palaeoclimatol., Palaeoecol. **238**, 281–301.

Ferguson DK, Hofmann C-C, Denk T. 1999 Taphonomy: field techniques in modem environments. In: Jones TP, Rowe NP (eds) Fossil Plants and Spores: modern techniques. London: Geological Society, 210–213.

Freitag, H. 1971 Die natürliche Vegetation Afghanistans. Vegetatio **22**, 285–344.

Freitag, H. 1982 Mediterranean character of the vegetation in the Hindukush Mts., and the relationship between sclerophyllous and laurophyllous forests. Ecol. mediterr. **8**, 381–388.

Gersonde R, Velitzelos E. 1978 Diatomeenpaläoökologie im Neogen-becken von Vegora N-W Mazedonien (vorläufige Mitteilung). Ann. Gèol. Pays Hellèn. 30, 373–382.

Greenwood DR, Archibald SB, Mathewes RW, Moss PT. 2005 Fossil biotas from the Okanagan Highlands, southern British Columbia and northeastern Washington State: climates and ecosystems across an Eocene landscape. Can. J. Earth Sci. **42**, 167–185.

Grimm GW, Bouchal JM, Denk T, Potts A. 2016 Fables and foibles: A critical analysis of the Palaeoflora database and the Coexistence Approach for palaeoclimate reconstruction. Rev. Palaeobot. Palyn. **233**, 611–622.

Grimm GW, Potts A. 2016 Fallacies and fantasies: the theoretical underpinnings of the Coexistence Approach for palaeoclimate reconstruction. Clim. Past **12**, 611–622.

Halbritter H, Ulrich S, Grímsson F, Weber M, Zetter R, Hesse M, Buchner R, Svojtka M, Frosch-Radivo A. 2018 Illustrated Pollen Terminology, 2nd ed. Cham (Switzerland): Springer Nature.

Herbert TD, Lawrence KT, Tzanova A, Peterson LC, Caballiero-Gill R, Kelly CS. 2016 Late Miocene global cooling and the rise of modern ecosystems. Nature Geosci. **9**, 843–847.

Hsü KJ, Ryan WBF, Cita MB. 1973 Late Miocene desiccation of the Mediterranean. Nature **242**, 240–244.

Ivanov DA. 2001 Palaeoecological interpretation of a pollen diagram from the Sandanski graben (Southwest Bulgaria). Comptes Rend. Acad. Bulg. Sci. **54**, 65–68.

Ivanov DA, Slavomirova E. 2002 Preliminary palynological data on Neogene flora from Bitola Basin (F.Y.R.O.M.). Comptes Rend. Acad. Bulg. Sci. **55**, 81–86.

Janis CM. 1986 An estimation of tooth volume and hypsodonty indices in ungulate mammals, and the correlation of these factors with dietary preference. In: DE Russell, JP Santoro, D Sigogneau-Russell (eds) Teeth revisited. Proc. 7th Int. Symp. Dental Morph. Mém. Mus. Nat. Hist. naturelle, Sér. C **53**, 367–387.

Jiang X-L, Hipp AL, Deng M, Su T, Zhou Z-K, Yan M-X. 2019 East Asian origins of European holly oaks (*Quercus* section *Ilex* Loudon) via the Tibet-Himalaya. J. Biogeogr. **46**, 2188–2202. doi.org/10.1111/jbi.13654

Jiménez-Moreno G, Popescu SM, Ivanov U, Suc J-P. 2007 Neogene flora, vegetation and climate dynamics in southeastern Europe and the northeastern Mediterranean. In Haywood WM, Gregory FJ, Schmidt DN (eds) Deep-Time Perspectives on Climate Change: Marrying the Signal from Computer Models and Biological Proxies. Micropalaeont. Soc., Spec. Publ. Geol. Soc., London, 503–516.

Karistineos N, Ioakim C. 1989 Palaeoenvironmental and palaeoclimatic evolution of the Serres Basin (N. Greece) during the Miocene. Palaeogeogr., Palaeoclimatol., Palaeoecol. **70**, 275–285.

Knobloch E, Velitzelos E. 1986a Die obermiozäne Flora von Likudi bei Elassona (Thessalien, Griechenland). Doc. Nat. **29**, 5–20.

Knobloch E, Velitzelos E. 1986b Die obermiozäne Flora von Prosilion bei Kozani (Sud-Mazedonien, Griechenland). Doc. Nat. **29**, 29–33.

Knobloch E, Velitzelos E. 1987 New leaf floras in the Neogene of Greece. Vest. Ustred. ústav Geol. **62**, 157–164.

Kottek M, Grieser J, Beck C, Rudolf B, Rubel F. 2006 World map of the Köppen-Geiger climate classification updated. Meteorol. Z. **15**, 259–263.

Koufos GD. 1982 *Hipparion crassum* Gervais, 1859 from the lignites of Ptolemais (Macedonia-Greece). Proc. Kon. Ned. Akad. Weten. B. **85**, 229–239.

Koufos GD. 2006 The Neogene mammal localities of Greece: Faunas, chronology and biostratigraphy. Hellen. J. Geosci. **41**, 183–214.

Koufos GD, Kostopoulos DS, Koliadimou KK. 1991 Un nouveau gisement de mammiferes dans le Villafranchien de Macedoine occidentale (Gréce). C. R. Acad. Sci. Paris, ser. II **313**, 831–836.

Kovar-Eder J. 2003 Vegetation dynamics in Europe during the Neogene. In: Reumer JWF, Wessels W (eds) Distribution and Migration of Tertiary mammals in Eurasia. A Volume in honour of Hans de Bruijn. Deinsea **10**, 373–392.

Kovar-Eder J, Kvaček Z, Martinetto E, Roiron P. 2006 Late Miocene to Early Pliocene vegetation of southern Europe (7–4 Ma) as reflected in the megafossil plant record. Palaeogeogr., Palaeoclimatol., Palaeoecol. **238**, 321–339.

Kozlowski G, Bétrisey S, Song Y. 2018 Wingnuts (*Pterocarya*) and walnut family. Relict trees: linking the past, present and future. Natural History Museum Fribourg: Switzerland.

Kvaček, Z. 2007. Do extant nearest relatives of thermophile European Cenozoic plant elements reliably reflect climatic signal? Palaeogeography, Palaeoclimatology, Palaeoecology **253**, 32–40.

Kvaček Z, Velitzelos D, Velitzelos E. 2002 Late Miocene Flora of Vegora Macedonia N. Greece. Athens: Koralis.

Maharramova E. 2015 Genetic diversity and population structure of the relict forest trees *Zelkova carpinifolia* (Ulmaceae) and *Pterocarya fraxinifolia* (Juglandaceae) in the South Caucasus. PhD Dissertation. Freie Universität Berlin.

Mai HD. 1995 Tertiäre Vegetationsgeschichte Europas. Stuttgart: Gustav Fischer.

Mai DH, Velitzelos E. 1992 Über fossile Pinaceen-Reste im Jungtertiär von Griechenland. Feddes Repert. **103**, 1–18.

Mai DH, Velitzelos E. 1997 Paläokarpologische Beiträge zur jungtertiären Flora von Vegora (Nordgriechenland). Feddes Repert. **108**, 507–526.

Marinova E, Harrison SP, Bragg F, Connor S, de Laet V, Leroy SAG, Mudie P, Atanassova J, Bozilova E, Caner H, Cordova C, Djamali M, Filipova-Marinova M, Gerasimenko N, Jahns S, Kouli K, Kotthoff U, Kvavadze E, Lazarova M, Novenko E, Ramezani E, Röpke A, Shumilovskikh L, Tanțău I, Tonkov S. 2018 Pollen-derived biomes in the Eastern Mediterranean–Black Sea–Caspian-Corridor. J. Biogeogr. **45**, 484–499.

Mavridis A, Skourtsis-Coroneou V, Tsaila-Monopoli S. 1977 Contribution to the geology of the sub-Pelagonian zone (Vourinos area, West Macedonia). 6th Colloquium on the Geology of the Aegean Region, Athens 1977, Inst. Geol. Mining Res., Vol**. I**, 175–195.

Mayer H, Aksoy, H. 1986 Wälder der Türkei. Stuttgart: Gustav Fischer.

Melinte-Dobrinescu MC, Suc J-P, Clauzon G, Popescu S-M, Armijo R, Meyer B, Biltekin D, Çağatay MN, Ucarkus G, Jouannic G,Fauquette S, Çakir Z. 2009 The Messinian salinity crisis in the Dardanelles region: chronostratigraphic constraints. Palaeogeogr. Palaeoclim. Palaeoecol. **278**, 24–39.

Mosbrugger V, Utescher T. 1997 The coexistence approach — a method for quantitative reconstructions of Tertiary terrestrial palaeoclimate data using plant fossils. Palaeogeogr., Palaeoclimatol., Palaeoecol. **134**, 61–86.

Ognjanova-Rumenova N. 2005 Upper Neogene siliceous microfossils from Pelagonia Basin (Balkan Peninsula). Geol. Carpathica **56**, 347–358.

Pavlides SB, Mountrakis DM. 1986 Neotectonics of the Florina–Vegoritis–Ptolemais Neogene Basin (NW Greece): an example of extensional tectonics of the greater Aegean area. Ann. Géol. Pays Hellen. **33**, 311–327.

Pavlides SB, Mountrakis DM. 1987 Extensional tectonics of northwestern Macedonia, Greece, since the late Miocene. J. Struct. Geol. 9 (4), 385–392.

Peel MC, Finlayson BL, McMahon TA. 2007 Updated world map of the Köppen-Geiger climate classification. Hydrol. Earth Syst. Sci., **11**, 1633–1644.

Popescu S-M, Biltekin D, Winter H, Suc J-P, Melinte-Dobrinescu MC, Klotz S, Rabineau M, Combourieu-Nebout N, Clauzon G, Deaconu F. 2010 Pliocene and Lower Pleistocene vegetation and climate changes at the European scale: Long pollen records and climatostratigraphy. Quatern. Int. **219**, 152–167.

Psilovikos A, Karistineos N. 1986 A depositional sedimentary model for the Neogene uraniferous lignites of the Serres graben, Greece. Palaeogeogr., Palaeoclimatol., Palaeoecol. **56**, 1–16.

Punt W, Hoen PP, Blackmore S, Nilsson RH, Le Thomas A. 2007 Glossary of pollen and spore terminology. Rev. Palaeobot. Palynol. **143**, 1–81.

Ratnam J, Bond WJ, Fensham RJ, Hoffmann WA, Archibald S, Lehmann CER, Anderson MT, Higgins SI, Sankaran M. 2011 When is a ‘forest’ a savanna, and why does it matter? Glob. Ecol. Biogeogr. **20**, 653–660.

Roberts S, Rassios A, Wright L, Vacondios I, Vrachatis G, GrivasE, Nesbitt RW, Neary CR, Moat T, Kostantopolou L. 1988 Structural controls on the location and form of the Vourinos chromite deposits. In: Boissonnas J, Omenetto P (eds) Mineral deposits within the European Community. Springer, Berlin Heidelberg New York, pp 249–266.

Rubel F, Brugger K, Haslinger K, Auer I. 2017 The climate of the European Alps: Shift of very high resolution Köppen-Geiger climate zones 1800–2100. Meteorol. Z., **26**, 115–125. https://doi.org/10.1127/metz/2016/0816.

Schneider W. 1992 Floral successions in the Miocene swamps and bogs of Central. Europe. Z. Geol.Wiss. **20**, 555–570.

Spicer RA. 2008 CLAMP. In: Gornitz V. Ed. Encyclopedia of Paleoclimatology and Ancient Environments. Dordrecht: Springer.

Steenbrink J, Van Vugt N. Hilgen FJ, Wijbrans JR, Meulenkamp JE. 1999 Sedimentary cycles and volcanic ash beds in the lower Pliocene lacustrine succession of Ptolemais

(NW Greece): discrepancy between 40Ar/39Ar and astronomical ages. Palaeogeogr., Palaeoclimatol., Palaeoecol. **152**, 283–303.

Steenbrink J, Van Vugt N, Kloosterboer-van Hoeve ML, Hilgen FJ. 2000 Refinement of the Messinian APTS from sedimentary cycle patterns in the lacustrine Lava section (Servia Basin, NW Greece). Earth Planet. Sci. Lett. **181**, 161–173.

Steenbrink J, Hilgen FJ, Krijgsman W, Wijbrans JR, Meulenkamp JE. 2006 Late Miocene to Early Pliocene depositional history of the intramontane Florina-Ptolemais-Servia Basin, NW Greece: Interplay between orbital forcing and tectonics. Palaeogeogr., Palaeoclimatol., Palaeoecol. **238**, 151–178.

Suc J-P. 1984 Origin and evolution of the Mediterranean vegetation and climate in Europe. Nature **307**, 429–432.

Suc J-P, Popescu S-M, Do Couto D, Clauzon G, Rubino J-L, Melinte-Dobrinescu MC, Quillévéré F, Brun J-P, Dumurdžanov N, Zagorchev I, Lesdić V, Tomić D, Sokoutis D, Meyer B, Macaleţ R, Jelen B, Rihelj H. 2015 Marine gateway vs. fluvial stream within the Balkans from 6 to 5 Ma. Mar. Pet. Geol. **66**, 231–245.

Suc J-P, Popescu SM, Fauquette S, Bessedik M, Jiménez-Moreno G, Taoufiq B, Zheng Z, Medail F, Klotz S. 2018 Reconstruction of Mediterranean flora, vegetation and climate for the last 23 million years based on an extensive pollen dataset. Ecol. mediterr. **44**, 53–85.

The NOW Community: New and old worlds database of fossil mammals (NOW), Licensed under CC BZ 4.0 Release 2008, available at: http://www.helsinki.fi/science/now/, last access: 09 April 2020.

Traverse A. 2007 Paleopalynology. Topics in Geobiology **28**. Dordrecht: Springer.

Utescher T, Bruch AA, Erdei B, François I, Ivanov D, Jacques FMB, Kern AK, Liu Y-SC, Mosbrugger V, Spicer RA. 2014 The Coexistence Approach—Theoretical background and practical considerations of using plant fossils for climate quantification. Palaeogeogr., Palaeoclimatol., Palaeoecol. **410**, 58–73.

Van de Weerd A. 1979 Early Ruscinian rodents and lagomorphs (Mammalia) from the lignites near Ptolemais (Macedonia, Greece). Proc. Kon. Nederl. Akad. Wet., B. **82**, 127–170.

Van Zeist W, Bottema S. 1991 Late Quaternary vegetation of the Near East. Beih. Tübinger Atlas Vord. Orient, Reihe A (Naturwiss.) **18**, 1–156.

Van Zeist W, Woldring H, Stapert, D. 1975 Late Quaternary vegetation and climate of southwestern Turkey. Palaeohist. **14**, 35–143.

Velitzelos D, Denk T. 2002 Leaf epidermal characteristics of late Tertiary conifers from Greece: taxonomic significance and limitations. 6th Europ. Paleobot. Palynol. Conf. Athens, Greece, Abstracts, 183–184.

Velitzelos D, Bouchal JM, Denk T. 2014 Review of the Cenozoic floras of Greece. Rev. Palaeobot. Palynol. **204**, 1–15.

Velitzelos E, Gregor H-J. 1985 Neue paläofloristische Befunde im Neogen Griechenlands. Doc. Nat. **25**, 1–4.

Velitzelos E, Krach JE, Gregor H-J, Geissert F. 1983 *Bolboschoenus vegorae* – ein Vergleich fossiler und rezenter Rhizomknollen der Strandbinse. Doc. Nat. **5**, 1–57.

Velitzelos E, Kvaček Z. 1999 Review of the late Miocene flora of Vegora western Macedonia, Greece. Acta Palaeobotanica, Suppl. 2 (Proceed. 5th EPPC) 419–427.

Velitzelos E, Petrescu I. 1981 Seltene pflanzliche Fossilien aus dem Braunkohlebecken von Vegora. Ann. géol. Pays hellén. **30**, 767–777.

Velitzelos E, Schneider HE. 1977 Jungtertiäre Pflanzenfunde aus dem Becken von Vegora in West-Makedonien (Griechenland). Ann. Mus. Goulandris **3**, 173–180.
Velitzelos E, Schneider HE. 1979 Jungtertiäre Pflanzenfunde aus dem Becken von Vegora in West-Mazedonien. 3. Mitteilung: Eine Fächerpalme (*Chamaerops humulis* L.). Ann. géol. Pays hellén. **29**, 796–799.
Wolfe JA. 1993 A method of obtaining climatic parameters from leaf assemblages. US Geol. Surv. Bull. **2040**, 1–73.
Woodward FI, Lomas MR, Kelly CK. 2004 Global climate and the distribution of plant biomes. Phil. Trans. R. Soc. Lond. B. **359**, 1465–1476.
Yang J, Spicer RA, Spicer TEV, Li C-S. 2011 'CLAMP Online': a new web-based palaeoclimate tool and its application to the terrestrial Paleogene and Neogene of North America. Palaeobiodiv. Palaeoenviron. **91**, 163–183.
Zetter R. 1989 Methodik und Bedeutung einer routinemäßigen kombinierten lichtmikroskopischen und rasterelektronenmikroskopischen Untersuchung fossiler Mikrofloren. Cour. Forschungsinst. Senck. **109**, 41–50.

Table and Figure Captions

Table 1. Köppen-Geiger climate categories.
Table 2. Plant taxa recorded from unit 1 (lignite seam) and unit 2 (blue marls) of the Vegora section.
Table 3. Palynomorph abundance of sample S115992.
Table 4. Estimated climate parameters for the pre-evaporitic Messinian of Vegora from two CLAMP calibration datasets and from CA.
Table 5. Vegetation types recognised for the pre-evaporitic Messinian of the Florina–Ptolemais–Servia Basin and its northern and southern extensions.

Figure 1. Fossil localities and lithological map of the Florina–Ptolemais–Servia Basin and its extensions to the north (Bitola Basin) and south (Likoudi Basin).
Map redrawn after Steenbrink et al. (1999, 2006), Ognjanova-Rumenova (2005), Ivanov (2001) and Koufos (2006). Fossil localities: (**1**) Bitola Basin, Republic of North Macedonia, PF. (**2**) Vegora Basin, MF and PF (**3**) Dytiko, VF. (**4**) Prosilio, MF. (**5**) Lava, MF. (**6**) Likoudi, MF. (**7**) Serres Basin. (2–7) Greece. (**8**) Sandanski Graben, Bulgaria, PF. Abbreviations: Bitola Basin (B), Florina sub-Basin (F), Ptolemais sub-Basin (P), Servia sub-Basin (S), Likoudi Basin (L). Plant macrofossils (MF), palynoflora (PF), vertebrate fossils (VF).
Figure 2. Lithology and polarity zones of the Vegora section (redrawn after Steenbrink et al., 2006). In the polarity column, black denotes normal and white reversed polarity; shaded portions indicate undetermined polarity. The lower normal polarity interval corresponds to Subchron C3An.2n and the upper to C3An.1n (after Steenbrink et al., 2006). Position of fossil bearing strata following Velitzelos and Schneider (1979) and Kvaček et al. (2002).
Figure 3. Light microscopy (LM) and scanning electron microscopy (SEM) micrographs of algae, fern and fern allies, and gymnosperm palynomorphs.
(a) *Botryococcus* sp. cf. *B. braunii*. (b) *Spirogyra* sp. 1/*Ovoidites elongatus*. (c) *Spirogyra* sp. 2/*Cycloovoidites cyclus*. (d–e) *Osmunda* sp., (d) EV, (e) PV. (f) *Cryptogramma* vel *Cheilanthes* sp./*Cryptogrammosporis magnoides*, PV. (g–h) *Pteris* sp./*Polypodiaceoisporites corrutoratus*, (g) PV, (h) DV. (i) Davalliaceae vel Polypodiaceae gen. indet./*Verrucatosporites alienus*, EV. (j) Monolete spore fam. indet./*Leavigatosporites*

haardti, EV. (k–l) Papillate Cupressaceae pollen/*Inaperturopollenites hiatus*. (m) *Abies* sp., EV. (n–o) *Cathaya* sp., (n) PV, (o) SEM detail, nanoechinate sculpturing of cappa (PRV). (p) *Cedrus* sp., EV. (q) *Pinus* subgenus *Pinus* sp., EV. (r) *Pinus* subgenus *Strobus* sp., EV. (s–t) *Tsuga* sp. 1, (s) PV, (t) monosaccus and corpus detail, PRV. (u–v) *Tsuga* sp. 2, (u) PV, (v) monosaccus and corpus detail, PRV.
Abbreviations: equatorial view (EV), polar view (PV), distal view (DV), proximal view (PRV). Scale bars 10 µm (LM, h, t, v), 1 µm (o).
Figure 4. LM and SEM micrographs of Poales, Vitales, Rosales, Fagales, Malpighiales, and Geraniales.
(a) *Typha* sp./*Tetradomonoporites typhoides*, tetrad, PV. (b–c) Poaceae gen. indet., EV, (c) exine detail, PRV. (d–e) Monocotyledonae indet., (d) PV, (e) PRV. (f–g) *Parthenocissus* sp., EV. (h) *Ulmus* vel *Zelkova* sp., PV. (I) *Fagus* sp., EV. (j–k) *Quercus* sect. *Cerris* sp., EV, (k) SEM detail, mesocolpium exine sculpturing. (l–m) *Quercus* sect. *Ilex* sp., EV, (m) SEM detail, mesocolpium exine sculpturing. (n–o) *Quercus* sect. *Quercus* sp., PV, (o) SEM detail, apocolpium exine sculpturing. (p–q) Castaneoideae gen. indet., EV, (q) SEM detail, mesocolpium exine sculpturing. (r) *Carya* sp., PV. (s) *Platycarya* sp., PV. (t) Engehardioideae gen. indet., PV. (u) *Alnus* sp., PV. (v) *Betula* sp., PV. (w) *Carpinus* sp., PV. (x) *Corylus* sp., PV. (y) *Salix* sp., EV. (z–aa) *Geranium* sp., (z) PV, (aa) clavae detail.
Abbreviations: equatorial view (EV), polar view (PV), proximal view (PRV). Scale bars 10 µm (LM, e, g), 1 µm (c, k, m, o, q, aa).
Figure 5. LM and SEM micrographs of Sapindales, Malvales, Caryophyllales, Cornales, Asterales, Dipsacales, and Apiales.
(a–b) *Cotinus* sp., EV. (c–d) *Pistacia* sp., (c) PV, (d) exine SEM detail. (e–f) *Acer* sp. 1, (e) PV, (f) mesocolpium SEM detail. (g–h) *Acer* sp. 2, (g) PV, (h) mesocolpium SEM detail. (i–j) *Craigia* sp., (i) PV, (j) apocolpium SEM detail. (k) Amaranthaceae/Chenopodioideae gen. indet. sp.1. (l) Amaranthaceae/Chenopodioideae gen. indet. sp.2. (m–n) Caryophyllaceae gen. indet. (o–p) *Nyssa* sp., (o) PV, (p) exine sculpturing and aperture SEM detail. (q–r) *Fraxinus* sp., (q) EV, (r) mesocolpium SEM detail. (s–t) *Olea* sp., EV. (u) Cichorioideae gen. indet., PV. (v) Asteraceae gen indet. sp. 1, PV. (w) Asteraceae gen indet. sp. 2, PV. (x–z) *Succisa* sp., (x–y) PV, (z) aperture SEM detail. (aa–bb) Apiaceae gen. indet. sp. 1, EV. (cc–dd) Apiaceae gen. indet. sp. 2, EV. (ee–ff) Angiosperm pollen fam. et gen. indet., (ee) EV, (ff) mesocolpium SEM detail.
Abbreviations: equatorial view (EV), polar view (PV). Scale bars 10 µm (LM, b, n, t, y, z, bb, dd), 1 µm (d, f, h, j, p, r, ff).
Figure 6. Palynomorph abundancies from sample S115992 based on 430 counted pollen and spores. Algae and unidentified angiosperm pollen excluded. (a) Ratio between pollen produced from arboreal and non-arboreal taxa. (b) Abundancies of woody gymnosperms and angiosperms and of herbaceous angiosperms and ferns. (c) Abundancy of woody and herbaceous angiosperms on dry and wet soils.
Figure 7. Coexistence-Approach diagram showing coexistence intervals for MAT and CMMT. MAT and CMMT climate ranges of relict taxa *a priori* excluded from the analysis are shown on the left side of the diagram.
Blue bars, coldest month mean temperature; red bars, 10–90 percentile climatic range (MAT); dark red extensions, full climatic range (MAT).
Figure 8. Köppen signal diagram for the macrofossil and pollen floras of Vegora.

To test and illustrate the stability of the climatic signal, gymnosperms (common alpine elements) and azonal elements (e.g. riparian or swamp vegetation) were excluded in some runs.

Supplementary Material

Supplementary Material Tables S1 - Climatic parameters of NLR

Table S1 (1). Fossil species and climatic parameters of the corresponding NLR (depending on the fossil-species and their botanical affinities, climate parameters of species, sections, subgenera, genera, or subfamilies are used as NLR).

Table S1 (2). Climatic parameters of NLR.

Supplementary Material Tables S2 - Köppen-Geiger climate type signatures.

Table S2 (1). Scored Köppen-Geiger signatures of all NLR species of the macrofossil and pollen flora of Vegora.

Tables S2 (2). Köppen-Geiger signature values and diagram of the macrofossil and pollen flora of Vegora.

Supplementary Material S3 - Systematic palaeobotany, descriptions, and additional figures of palynomorphs from the plant fossil bearing strata of Vegora (sample S115992).

Supplementary Material Tables S4 - Palynomorph abundance of sample S115992.

Supplementary Material S5 - Coding of leaf physiognomic characters for morphotypes from the Vegora lignite mine macroflora. Output PDF files from online CLAMP analysis (http://clamp.ibcas.ac.cn).

Table 1. Köppen-Geiger climate categories.

Descripton of Köppen-Geiger climate symbols and defining criteria (Kottek et al., 2006; Peel et al., 2007)			
1st	2nd	3rd	Description and criteria
A			Equatorial / Tropical ($T_{cold} \geq 18°C$)
	f		Rainforest, fully humid ($P_{dry} \geq 60$ mm)
	m		Monsoonal (not *Af* & $P_{dry} \geq 100–MAP/25$)
	s		Savannah with dry summer ($P_{sdry} < 60$ mm)
	w		Savannah with dry winter ($P_{wdry} < 60$ mm)
B			Arid (MAP < 10 x $P_{threshold}$)
	W		Desert (MAP < 5 x $P_{threshold}$)
	S		Steppe (MAP ≥ 5 x $P_{threshold}$)
		h	Hot arid (MAT ≥ 18°C)
		k	Cold arid (MAT < 18°C)
C			Warm temperate / Temperate ($T_{hot} > 10°C$ & $0°C < T_{cold} < 18°C$
D			Snow / Cold ($T_{hot} > 10°C$ & $T_{cold} \leq 0°C$)
	s		Summer dry ($P_{sdry} < 40$ mm & $P_{sdry} < P_{wwet}/3$
	w		Winter dry ($P_{wdry} < P_{swet}/10$)
	f		Fully humid / without a dry season (not *s* or *w*)
		a	Hot summer ($T_{hot} \geq 22°C$)
		b	Warm summer (not *a* & $T_{mon10} \geq 4$)
		c	Cool / cold summer (not *a* or *b* & $T_{cold} > -38°C$)
		d	Extremely continental / very cold winter (not *a* or *b* & $T_{cold} \leq -38°C$)
E			Polar ($T_{hot} < 10°C$)
	T		Polar tundra ($T_{hot} \leq 10°C$)
	F		Polar frost ($T_{hot} \leq 0°C$)

MAP = mean annual precipitation, MAT = mean annual temperature, T_{hot} = temperature of the hottest month, T_{cold} = temperature of the coldest month, T_{mon10} = number of months where the temperature is above 10°C, P_{dry} = precipitation of the driest month, P_{sdry} = precipitation of the driest month in summer, P_{wdry} = precipitation of the driest month in winter, P_{swet} = precipitation of the wettest month in summer, P_{wwet} = precipitation of the wettest month in winter, $P_{threshold}$ = varies according to the following rules (if 70% of MAP occurs in winter then $P_{threshold}$ = 2 x MAT, if 70% of MAP occurs in summer then $P_{threshold}$ = 2 x MAT + 28, otherwise $P_{threshold}$ = 2 x MAT + 14). Summer (winter) is defined as the warmer (cooler) six months period of ONDJFM and AMJJAS.

Table 2. Plant taxa recorded from unit 1 (lignite seam) and unit 2 (blue marls) of the Vegora section.

Vegora micro, meso and macro flora					
Taxon	**Element**	**Reference**	**Life form**	**Ecology**	**Vegetation units [BLD subgroups]** [a]
Algae					
Botryococcaceae					
Botryococcus sp.	P	11	Algae	Aquatic	**VU1**
Zygnemataceae					
Spirogyra spp.	P	11	Algae	Aquatic	**VU1**
Fern and fern allies					
Osmundaceae					
Osmunda sp.	P	11	Fern	Swamp, riparian, well-drained lowland forest	**VU3, VU4, VU5**
Osmunda parschlugiana	L	2, 8	Fern	Swamp, riparian, well-drained lowland forest	**VU3, VU4, VU5**
Polypodiaceae					
Cryptogramma vel *Cheilanthes* sp.	P	11	Fern	Swamp, riparian, well-drained lowland forest	**VU3, VU4, VU5**
Pteridaceae					
Pteris sp.	P	11	Fern	Swamp, riparian, well-drained lowland forest	**VU3, VU4, VU5**
Fam. incerta sedis					
Davalliaceae vel Polypodiaceae gen. indet.	P	11	Fern	Swamp, riparian, well-drained lowland forest	**VU3, VU4, VU5**
Laevigatosporites haardti	P	11	Fern	Swamp, riparian, well-drained lowland forest	**VU3, VU4, VU5**
Gymnosperms					
Ginkgoaceae	L				
Ginkgo adiantoides	L	8, 9	$Tree_{gym}$	Riparian forests	**VU4**
Cupressaceae					
Cupressus rhenana	L, R	6, 8	$Tree_{gym}$	Conifer forest lowland, upland, peat-forming	**VU7**
Sequoia abietina	L	8, 10	$Tree_{gym}$	Conifer forest lowland, upland, peat-forming	**VU7**
Cryptomeria anglica	L	10	$Tree_{gym}$	Conifer forest lowland, upland, peat-forming	**VU7**
Glyptostrobus europaeus	L, R	6, 8	$Tree_{gym}$	Swamp forest	**VU3**
Taxodium dubium	L, R	6, 8	$Tree_{gym}$	Swamp forest	**VU3**
Papillate Cupressaceae	P	11	$Tree_{gym}$	Indifferent	
Pinaceae					
Abies sp.	P	11	$Tree_{gym}$	Well-drained lowland and upland forests	**VU5, VU6, VU7**
Cathaya sp.	P	11	$Tree_{gym}$	Conifer forest lowland, upland, peat-forming	**VU7**
Cedrus sp.	P	11	$Tree_{gym}$	Well-drained lowland and upland forests	**VU7**
Cedrus vivariensis	R	4, 8	$Tree_{gym}$	Well-drained lowland and upland forest	**VU7**
Keteleeria hoehnei	R	6	$Tree_{gym}$	Conifer forest lowland, upland, peat-forming	**VU7**
Pinus hampeana (diploxylon)	R	6, 8	$Tree_{gym}$	Well-drained lowland forest	**VU5**
Pinus salinarum (diploxylon)	R	4, 8	$Tree_{gym}$	Well-drained lowland forest	**VU5**
Pinus spp.	L, R	8	$Tree_{gym}$	Indifferent	
Pinus sp. diploxylon type	P	11	$Tree_{gym}$	Indifferent	
Pinus sp. haploxylon type	P, R	8, 11	$Tree_{gym}$	Indifferent	
Pinus vegorae (haplox.)	R	4, 6	$Tree_{gym}$	Well-drained lowland forest	**VU5**
Tsuga spp.	P	11	$Tree_{gym}$	Conifer forest lowland, upland, peat-forming	**VU7**
Angiosperms					
Cabombaceae					
Brasenia sp.	R	4	Herb	Aquatic	**VU1**
Lauraceae					
Daphnogene pannonica	L	8	Tree	Well-drained lowland forest	**VU5 [BLD $_{wet}$]**
Laurophyllum pseudoprinceps	L	8	Tree	Well-drained lowland forest	**VU5 [BLD $_{wet}$]**
Sassafras ferrettianum	L	7, 8	Tree	Riparian, well-drained lowland forest	**VU4, VU5 [BLD wet]**
Laurophyllum sp.	L	8	Tree	Indifferent	**[BLD wet]**
Potamogetonaceae					
Potamogeton sp.	R	4	Herb	Aquatic	**VU1**
Arecaceae					
Chamaerops humilis fossilis	L	1, 8	Palm	Well-drained lowland forest or scrub	**VU0, VU5 [BLD $_{drought}$]**
Zingiberaceae					
Spirematospermum wetzleri	R	4	Herb	Bogs, wet meadows	**VU2**
Typhaceae					
Typha sp.	P	11	Herb	Aquatic, bogs, swamp forest, riparian forest	**VU1, VU2, VU3, VU4**
Poaceae					
Poaceae gen. indet.	P	11	Herb	Indifferent	
Cyperaceae					
Bolboschoenus vegorae	R	3, 4	Herb	Meadows	**VU2**

Cladium	R	4	Herb	Bogs, wet meadows	**VU2**
Ceratophyllaceae					
Ceratophyllum sp.	R	4	Herb	Aquatic	**VU1**
Platanaceae					
Platanus leucophylla	L	8	Tree	Riparian, well-drained lowland forest	**VU4, VU5 [BLD $_{drought}$]**
Vitaceae					
Parthenocissus sp.	P	11	Liana	Swamp forest, riparian, well-drained lowland forest	**VU3, VU4, VU6**
Fabaceae					
Leguminosites sp.	L	8	Tree	Indifferent	**[BLD]**
Ulmaceae					
Ulmus vel *Zelkova*	P	11	Tree	Riparian, well-drained lowland forest	**VU0, VU4, VU5 [BLD]**
Ulmus plurinervia	L	8	Tree	Riparian, well-drained lowland forest	**VU4, VU5 [BLD $_{cold}$]**
Zelkova zelkovifolia	L	8	Tree	Mediterranean scrub, riparian, well-drained lowland forest	**VU0, VU4, VU5 [BLD $_{drought}$]**
Fagaceae					
Castaneoideae gen indet.	P	11	Tree	Well-drained lowland forest	**VU5 [BLD]**
Castanea sp.	R	6, 8	Tree	Well-drained lowland forest	**VU5 [BLD]**
Fagus sp.	P	11	Tree	Well-drained lowland and upland forest	**VU5, VU5 [BLD $_{cold}$]**
Fagus gussonii	L, R	6, 7, 8	Tree	Well-drained lowland and upland forest	**VU5, VU6 [BLD $_{cold}$]**
Quercus sect. *Cerris*	P	11	Tree	Well-drained lowland forest	**VU5 [BLD]**
Quercus cerrisaecarpa	R	6, 8	Tree	Well-drained lowland forest	**VU5 [BLD]**
Quercus gigas	L	7, 8	Tree	Well-drained lowland forest	**VU5 [BLD]**
Quercus kubinyii	L	8	Tree	Well-drained lowland forest	**VU5 [BLD $_{drought}$]**
Quercus sect. *Ilex*	P	11	Tree	Mediterranean scrub, well-drained lowland forest	**VU0, VU5 [BLD $_{drought}$]**
Quercus drymeja	L	7, 8	Tree	Well-drained lowland and upland forests	**VU5, VU6 [BLD $_{drought}$]**
Quercus mediterranea	L	7, 8	Tree	Mediterranean scrub, well-drained lowland forest	**VU0, VU5 [BLD $_{drought}$]**
Quercus sosnowskyi	L	7, 8	Tree	Well-drained lowland forest	**VU5 [BLD $_{drought}$]**
Quercus sect. *Quercus*	P	11	Tree	Riparian forest, well-drained lowland forest	**VU4, VU5 [BLD]**
Quercus pseudocastanea	L	8	Tree	Well-drained lowland forest	**VU5 [BLD$_{cold}$]**
Quercus sp.	R	8	Tree	Indifferent	**[BLD]**
Juglandaceae					
Carya sp.	P	11	Tree	Riparian, well-drained lowland forest	**VU4, VU5 [BLD]**
Platycarya sp.	P	11	Tree	Riparian, well-drained lowland forest	**VU4, VU5 [BLD]**
Pterocarya paradisiaca	L	7, 8	Tree	Riparian, well-drained lowland forest	**VU4, VU5 [BLD]**
Engelhardioideae gen. indet.	P	11	Tree	Riparian, well-drained lowland forest	**VU4, VU5 [BLD]**
Betulaceae					
Alnus sp.	P	11	Tree	Swamp, riparian forest, well-drained lowland forest	**VU3, VU4, VU5 [BLD $_{cold}$]**
Alnus adscendens	L	8	Tree	Well-drained lowland forest	**VU5 [BLD $_{cold}$]**
Alnus cecropiifolia	L	8	Tree	Swamp, riparian forest	**VU3, VU4 [BLD $_{cold}$]**
Alnus cf. *kefersteinii*	R	6, 8	Tree	Indifferent	**[BLD $_{cold}$]**
Alnus ducalis	L	7, 8	Tree	Well-drained lowland forest	**VU5 [BLD $_{cold}$]**
Alnus gaudinii	L	8	Tree	Well-drained lowland forest	**VU5 [BLD $_{cold}$]**
Alnus julianiformis	L	8	Tree	Riparian, well-drained lowland forest	**VU4, VU5 [BLD $_{cold}$]**
Betula sp.	P	11	Tree	Riparian, well-drained lowland and upland forest	**VU4, VU5, VU6 [BLD $_{cold}$]**
Betula pseudoluminifera	L	8	Tree	Well-drained lowland forest	**VU5 [BLD $_{cold}$]**
Carpinus sp.	P	11	Tree	Well-drained lowland forest	**VU5 [BLD]**
Carpinus betulus fossilis	R	8	Tree	Well-drained lowland forest	**VU5 [BLD]**
Carpinus grandis	L	8	Tree	Well-drained lowland forest	**VU5 [BLD]**
Carpinus kisseri, group of *C. tschonoskii*	R	6, 8	Tree	Well-drained lowland forest	**VU5 [BLD]**
Corylus sp.	P	11	Shrub	Well-drained lowland forest	**VU5 [BLD]**
Salicaceae					
Populus balsamoides	L	8	Tree	Riparian forest	**VU4 [BLD]**
Populus populina	L	8	Tree	Riparian forest	**VU4 [BLD]**
Populus spp.	L	7, 8	Tree	Riparian forest	**VU4 [BLD]**
Salix sp.	P	11	Tree	Swamp, riparian forest	**VU3, VU4 [BLD]**
Geraniaceae					
Geranium sp.	P	11	Herb	Steppe, meadows, well-drained lowland forest	**VU0, VU2, VU5**
Lythraceae					
Decodon globosus	R	4	Shrub	Swamp	**VU3**
Anacardiaceae					
Cotinus sp. (=*Dicotylophyllum* sp. 5)	L, P	8, 11	Shrub	Well-drained lowland forest	**VU5 [BLD $_{drought}$]**
Pistacia sp.	P	11	Tree, shrub	(Mediterranean) scrub, well-drained lowland forest	**VU0, VU5**
Sapindaceae					
Acer aegopodifolium	L	7, 8	Tree	Well-drained lowland and upland forests	**VU5, VU6 [BLD]**
Acer integrilobum	L	8	Tree	Well-drained lowland and upland forests	**VU5, VU6 [BLD]**
Acer limburgense (sect. *Macrophylla*)	R	6, 8	Tree	Well-drained lowland and upland forests	**VU5, VU6 [BLD]**
Acer pseudomonspessulanum	L	8	Tree	(Mediterranean) scrub, well-drained lowland forest	**VU0, VU5 [BLD $_{drought}$]**
Acer pyrenaicum (sect. *Rubra)*	L	7, 8	Tree	Well-drained lowland forest	**VU5 [BLD]**

Acer subcampestre	L	8	Tree	Well-drained lowland and upland forest	**VU5, VU6 [BLD $_{drought}$]**
Acer tricuspidatum (sect. *Rubra*)	L	8	Tree	Swamp, well-drained lowland and upland forest	**VU3, VU5, VU6 [BLD $_{cold}$]**
Acer spp.	P, R	8, 11	Tree	Indifferent	**[BLD]**
Malvaceae					
Craigia sp.	P	11	Tree	Well-drained lowland forest	**VU5 [BLD]**
Craigia bronnii	R	6, 8	Tree	Well-drained lowland forest	**VU5 [BLD]**
Droseraceae					
Aldrovandia praevesiculosa	R	4	Herb	Aquatic	**VU1**
Caryophyllaceae					
Caryophyllaceae gen. indet.	P	11	Herb	Steppe, meadows, well-drained lowland and upland forest	**VU0, VU2, VU5, VU6**
Amaranthaceae					
Amaranthaceae/Chenopodiaceae gen. indet. spp.	P	11	Herb	Steppe, meadows	**VU0, VU2**
Nyssaceae					
Nyssa sp.	P	11	Tree	Swamp, well-drained lowland and upland forest	**VU3, VU5, VU6 [BLD $_{wet}$]**
Oleacaee					
Fraxinus sp.	R, P	8, 11	Tree	Riparian forest	**VU4 [BLD]**
Olea sp.	P	11	Tree	Mediterranean scrub, well-drained lowland forest	**VU0, VU5**
Asteraceae					
Asteraceae gen. indet. spp.	P	11	Herb	Steppe, meadows, well-drained lowland and upland forest	**VU0, VU2, VU5, VU6, VU7**
Cichorioideae gen. indet.	P	11	Herb	Steppe, meadows, well-drained lowland and upland forest	**VU0, VU2, VU5, VU6, VU7**
Caprifoliaceae					
Succisa sp.	P	11	Herb	Steppe, meadow, riparian	**VU0, VU2, VU4**
Araliaceae					
Hedera multinervis	L	7, 8	Liana	Riparian, well-drained lowland forest	**VU4, VU5**
Apiaceae					
Apiaceae gen. indet. spp.	P	11	Herb	Steppe, meadows, well-drained lowland and upland forest	**VU0, VU2, VU5, VU6, VU7**
Incerta sedis					
Monocotyledone indet.	L	8	Herb	Swamp, riparian, lake margin	**VU2, VU3, VU4**
Dicotylophyllum sp. 1–4, 6	L	8			
Monocotyledone indet.	P	11			
Pollen indet.	P	11			

[a]BLD (Broadleaf deciduous forest biome of Woodward et al., 2004) was divided in BLD drought, deciduous trees and shrubs that are drought resistant, and BLD cold, deciduous trees and shrubs that are cold tolerant; in addition we use BLD wet for trees and shrubs that typically occur in humid warm temperate regions.

Vegetation Unit **(VU) 0**: Steppe-like meadows with shrubs and/or small trees scattered or in groups; Mediterranean scrub. **VU 1**: Aquatic. **VU 2**: Bogs, wet meadows. **VU 3**: Swamp forest. **VU 4**: Riparian forest. **VU 5**: Well-drained lowland forest **-a** ''hot''(Lauraceae,*Chamaerops,* Engelhardioideae, *Olea*); **-b** ''temperate'' (*Castanea*, *Carpinus*, *Tilia*) including levee forests. **VU 6**: Well-drained upland forest (**-a** *Quercus drymeja-mediterranea*; **-b** *Fagus-Cathaya*). **VU 7**: Well-drained (lowland and) upland conifer forest including hammocks and raised bogs within peat-forming vegetation. Vegetation units from Denk (2016).

Abbreviations: leaves (L); palynomorph (P); reproductive structures (R).

References: 1) Velitzelos & Schneider, 1979; 2) Velitzelos & Petrescu, 1981; 3) Velitzelos et al., 1983; 4) Velitzelos & Gregor, 1985; 5) Mai & Velitzelos, 1992; 6) Mai & Velitzelos, 1997; 7) Velitzelos & Kvaček, 1999; 8) Kvaček et al., 2002; 9) Denk & Velitzelos, 2002; 10) Velitzelos & Denk, 2002; 11) this study

Table 3. Palynomorph abundance of sample S115992.

Taxon	Count
Pinus subgen. *Strobus*	47
Alnus sp.	40
Abies sp.	36
Cathaya sp.	30
Fagus sp.	30
Pinus subgen. *Pinus*	33
Quercus sp. (large)	21
Papillate Cupressaceae	19
Spirogyra sp.	18
Osmunda sp.	18
Ulmus vel *Zelkova* sp.	18
Cedrus sp.	18
Carya sp.	13
Engelhardioideae gen. indet.	10
Quercus sp. (small)	9
Betula sp.	8
Salix sp.	8
Leavigatosporites haardti	7
Tsuga sp.	7
Amaranthaceae gen. indet. sp.	3
Apiaceae spp.	3
Carpinus sp.	3
Olea sp.	3
Davalliaceae vel Polypodiaceae gen. indet.	2
Asteroideae gen. indet. sp.	2
Typha sp.	2
Corylus sp.	2
Acer sp.	2
Nyssa sp.	2
Incertae sedis	2
Cryptogramma vel *Cheilanthes* sp.	1
Pteris sp.	1
Poaceae gen. indet. sp.	1
Geranium sp.	1
Caryophyllaceae gen. indet.	1
Cichorioideae gen. indet.	1
Succisa sp.	1
Parthenocissus sp.	1
Castaneoideae gen. indet.	1
Platycarya sp.	1
Cotinus sp.	1
Pistacia sp.	1
Craigia sp.	1
Fraxinus sp.	1
Sum of counted grains and spores	430

Table 4. Estimated climate parameters for the pre-evaporitic Messinian of Vegora from two CLAMP calibration datasets and from CA.

Climate parameter	CLAMP Physg3arcAZ	CLAMP PhysgAsia1	CA modified	CA modified 10-90%iles
MAT (°C)	10–13.5	8.7–11.5	8.6–21.2	9.9–18.4
CMMT (°C)	1–5	-2.7–2.3	≥ 1.2	-
WMMT (°C)	19.2–22.8	19–22.6	-	-
GROWSEAS (months)	6–8	5.5–7	-	-
MMGSP (mm)	110–160	100–160	-	-
Three_WET (mm)	500–780	400–750	-	-
Three_DRY (mm)	180–260	80–220	-	-
3_WET/3_DRY	< 4	< 5.5	-	-

MAT = mean annual temperature, CMMT = coldest month mean temperature, WMMT = warmest month mean temperature, GROWSEAS = duration of growing season, MMGSP = mean month growing season precipitation, Three_WET = precipitation of three consecutive wettest months, Three_DRY = precipitation of three consecutive driest months.

Table 5. Vegetation types recognised for the pre-evaporitic Messinian of the Florina–Ptolemais–Servia Basin.

Vegetation type	Main (and accessory) taxon/taxa	Biome[a]	Vegetation unit(s)[b]	Modern (Neogene) analogue	References
Swamp forest	*Taxodium* , *Glyptostrobus*	NLD	VU3	*Taxodium* swamp forests SE USA; (*Taxodium/Glyptostrobus* swamp forests widespread in N Hemisphere Neogene)	1, 2
Swamp forest	*Alnus* , (*Sassafras*)	BLD	VU3	*Alnus* swamp forest	3, 4
Riparian forest	*Pterocarya* , *Zelkova* , *Ulmus* , (*Sassafras*)	BLD	VU4	Riparian and alluvial forest of Georgia and Iran	1, 3, 4, 5, 6
Well-drained forest	*Quercus kubinyi* , *Q. pseudocastanea* , (*Carpinus* , *Tilia* etc.)	BLD	VU5b	Lowland oak-hornbeam forests; ("Quercetum mixtum")	4, 7
Well-drained forest	*Fagus* , (*Quercus pseudocastanea*)	BLD	VU5b	Lowland beech forests of N Turkey, Georgia, N Iran; ("Fagetum gussonii")	3, 4, 7
Well-drained forest	*Fagus* , *Abies* , *Cedrus* , *Cathaya*	MIXED	VU6b	Montane *Fagus-Abies* forest, montane *Fagus-Cedrus-Pinus* forest; Abant Gölü; Erbaa-Çatalan	8, 9, 10
Well-drained laurophyllous forest	*Quercus drymeja* , (*Q. sosnowsky*)	BLE	VU6a	*Quercus dilatata* association (with *Taxus* , *Pinus* , *Acer* etc.)	11
Well-drained sclerophyllous forests/shrublands	*Quercus mediterranea* , *Chamaerops* , *Olea*	BLE/ SHRUBLAND	VU0	Mediterranean sclerophyllous forest/shrublands	10
[?][c] Grassland-steppe forest	Poaceae	GRASSLAND/ SHRUBLAND	VU0	Forest-steppe of SE Europa to Afghanistan	8, 10, 11, 12

1) Mai, 1995; 2) Dolezych & Schneider, 2007; 3) Denk et al., 2001; 4) Akhani et al., 2010; 5) Maharramova, 2015; 6) Kozlowski et al., 2018; 7) Kvaček et al., 2002; 8) Mayer & Aksoy, 1986; 9) Akkemik, 2003; 10) van Zeist & Bottema, 1991; 11) Freitag, 1971; 12) Erdős et al., 2018

[a]Biome classification follows the phsiognomic approach of Woodward et al., 2004. [b]Vegetation units as in Table 1.

[c] [?] expresses the uncertainty around a possible extra-regional signal in the Vegora pollen record. According to Erdös et al. (2018) steppe forest with *Stipa* and other grasses and different species of *Quercus* (forest-steppes of the type 'Region A - SE Europe') is characterized by MAP of 420–600 mm; this would be much drier than the inferred MAP for the FPS.

Figure 1.

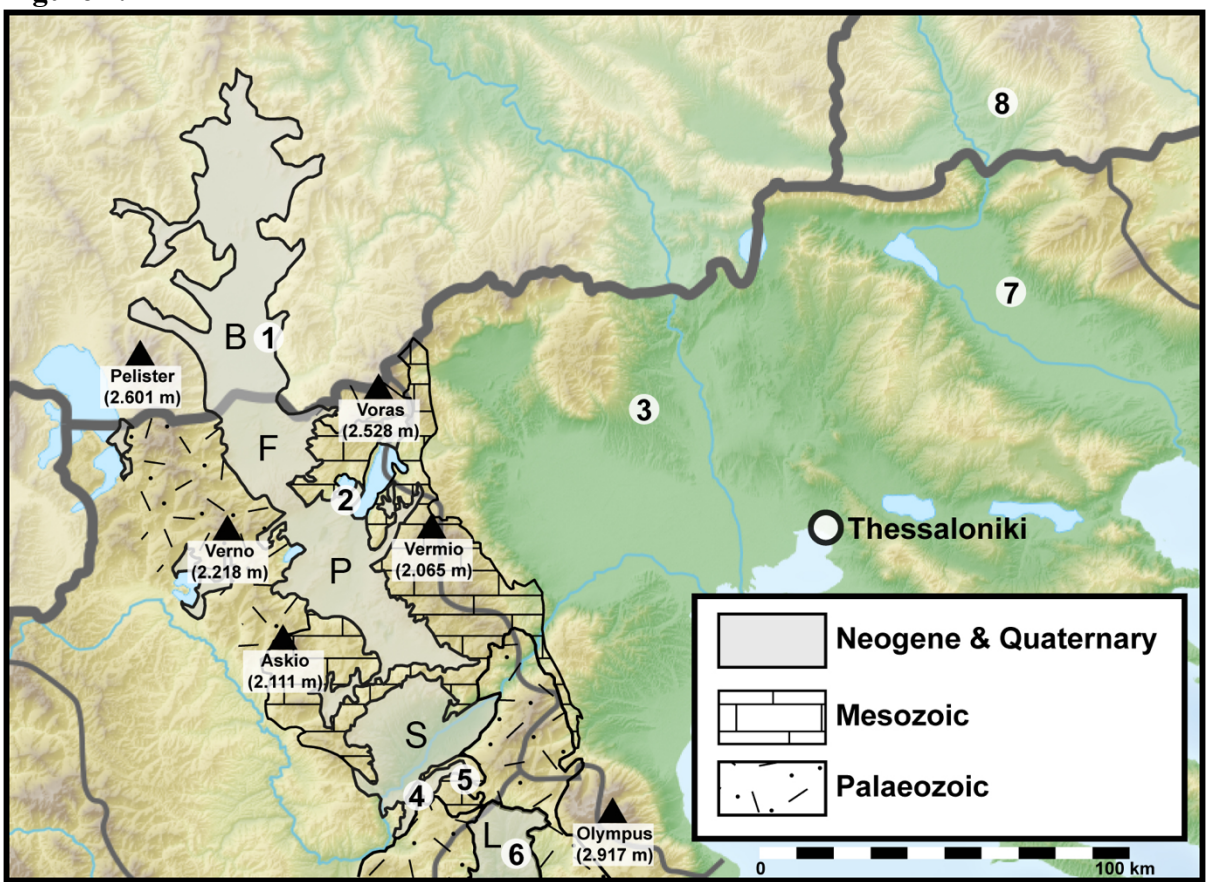

Figure 1. Fossil localities and lithological map of the Florina–Ptolemais–Servia Basin and its extensions to the north (Bitola Basin) and south (Likoudi Basin).
Map redrawn after Steenbrink et al. (1999, 2006), Ognjanova-Rumenova (2005), Ivanov (2001) and Koufos (2006). Fossil localities: (**1**) Bitola Basin, Republic of North Macedonia, PF. (**2**) Vegora Basin, MF and PF (**3**) Dytiko, VF. (**4**) Prosilio, MF. (**5**) Lava, MF. (**6**) Likoudi, MF. (**7**) Serres Basin. (2–7) Greece. (**8**) Sandanski Graben, Bulgaria, PF. Abbreviations: Bitola Basin (B), Florina sub-Basin (F), Ptolemais sub-Basin (P), Servia sub-Basin (S), Likoudi Basin (L). Plant macrofossils (MF), palynoflora (PF), vertebrate fossils (VF).

Figure 2

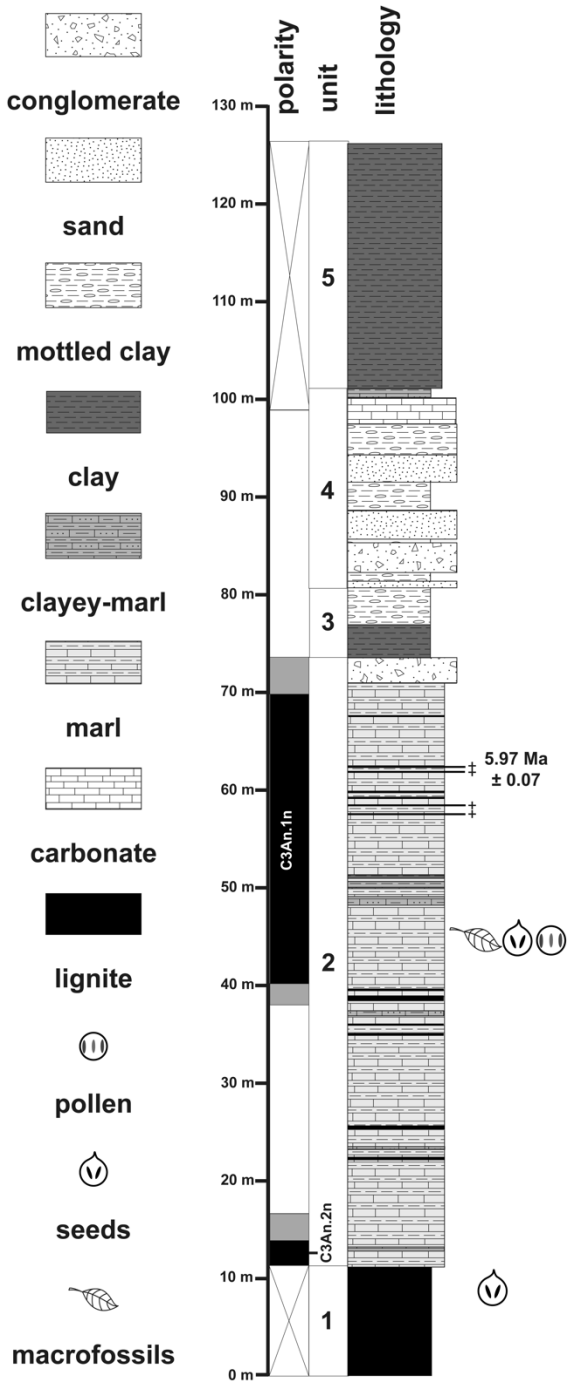

Figure 2. Lithology and polarity zones of the Vegora section (redrawn after Steenbrink et al., 2006). In the polarity column, black denotes normal and white reversed polarity; shaded portions indicate undetermined polarity. The lower normal polarity interval corresponds to Subchron C3An.2n and the upper to C3An.1n (after Steenbrink et al., 2006). Position of fossil bearing strata following Velitzelos and Schneider (1979) and Kvaček et al. (2002).

Figure 3.

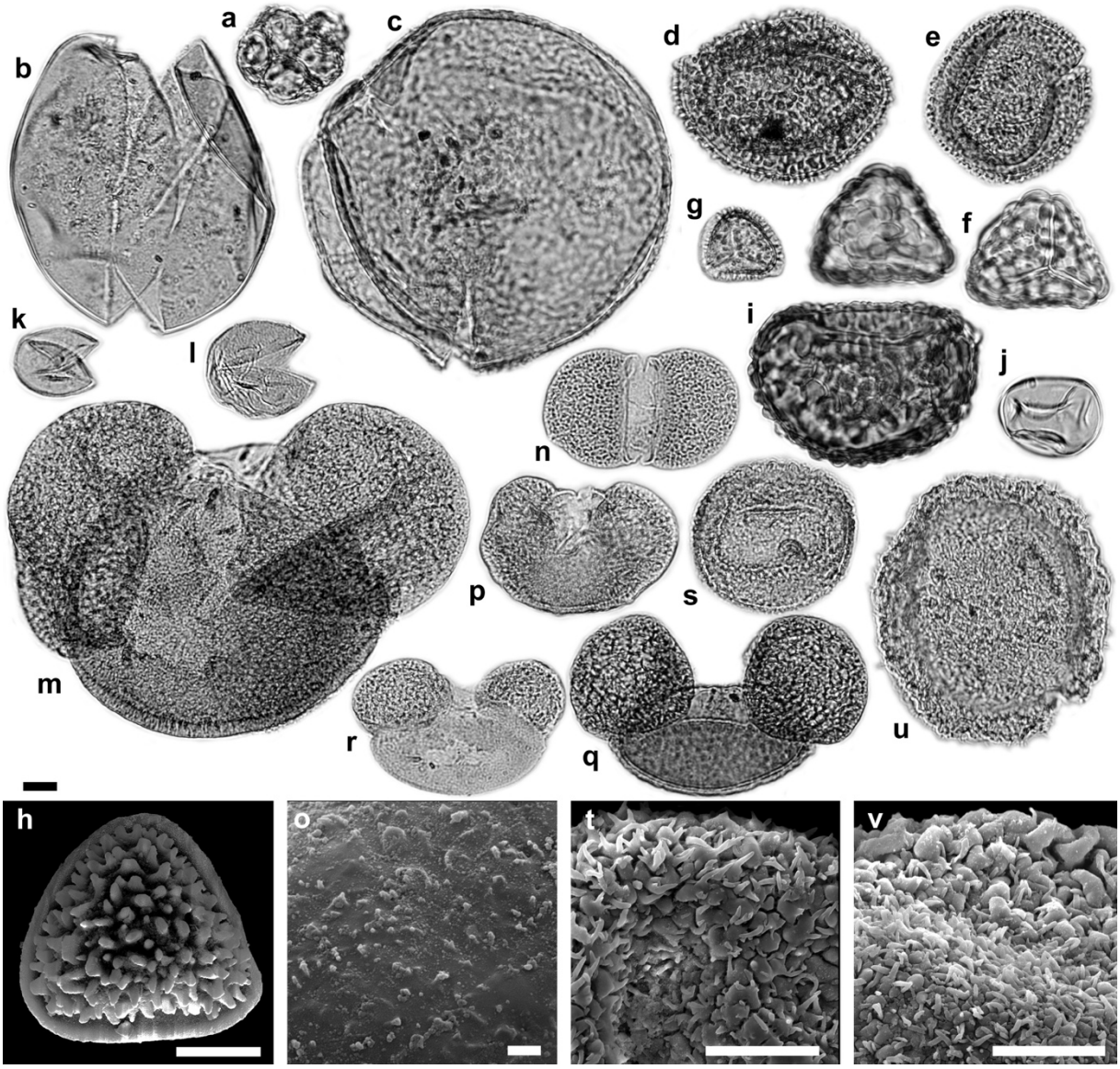

Figure 3. Light microscopy (LM) and scanning electron microscopy (SEM) micrographs of algae, fern and fern allies, and gymnosperm palynomorphs.
(a) *Botryococcus* sp. cf. *B. braunii*. (b) *Spirogyra* sp. 1/*Ovoidites elongatus.* (c) *Spirogyra* sp. 2/*Cycloovoidites cyclus.* (d–e) *Osmunda* sp., (d) EV, (e) PV. (f) *Cryptogramma* vel *Cheilanthes* sp./*Cryptogrammosporis magnoides*, PV. (g–h) *Pteris* sp./*Polypodiaceoisporites corrutoratus*, (g) PV, (h) DV. (i) Davalliaceae vel Polypodiaceae gen. indet./*Verrucatosporites alienus*, EV. (j) Monolete spore fam. indet./*Leavigatosporites haardti*, EV. (k–l) Papillate Cupressaceae pollen/*Inaperturopollenites hiatus*. (m) *Abies* sp., EV. (n–o) *Cathaya* sp., (n) PV, (o) SEM detail, nanoechinate sculpturing of cappa (PRV). (p) *Cedrus* sp., EV. (q) *Pinus* subgenus *Pinus* sp., EV. (r) *Pinus* subgenus *Strobus* sp., EV. (s–t) *Tsuga* sp. 1, (s) PV, (t) monosaccus and corpus detail, PRV. (u–v) *Tsuga* sp. 2, (u) PV, (v) monosaccus and corpus detail, PRV.
Abbreviations: equatorial view (EV), polar view (PV), distal view (DV), proximal view (PRV). Scale bars 10 µm (LM, h, t, v), 1 µm (o).

Figure 4.

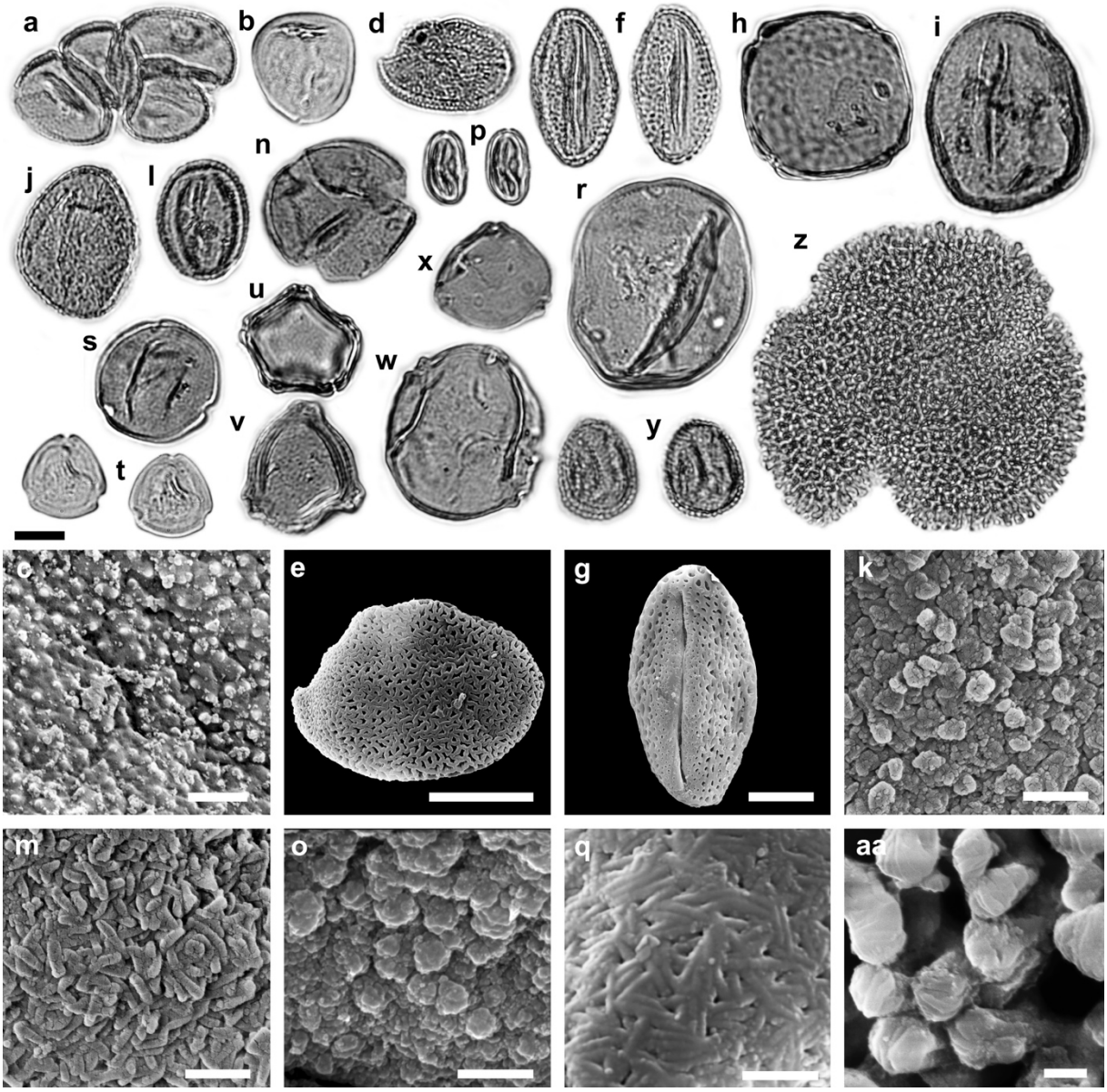

Figure 4. LM and SEM micrographs of Poales, Vitales, Rosales, Fagales, Malpighiales, and Geraniales.
(a) *Typha* sp./*Tetradomonoporites typhoides*, tetrad, PV. (b–c) Poaceae gen. indet., EV, (c) exine detail, PRV. (d–e) Monocotyledonae indet., (d) PV, (e) PRV. (f–g) *Parthenocissus* sp., EV. (h) *Ulmus* vel *Zelkova* sp., PV. (I) *Fagus* sp., EV. (j–k) *Quercus* sect. *Cerris* sp., EV, (k) SEM detail, mesocolpium exine sculpturing. (l–m) *Quercus* sect. *Ilex* sp., EV, (m) SEM detail, mesocolpium exine sculpturing. (n–o) *Quercus* sect. *Quercus* sp., PV, (o) SEM detail, apocolpium exine sculpturing. (p–q) Castaneoideae gen. indet., EV, (q) SEM detail, mesocolpium exine sculpturing. (r) *Carya* sp., PV. (s) *Platycarya* sp., PV. (t) Engehardioideae gen. indet., PV. (u) *Alnus* sp., PV. (v) *Betula* sp., PV. (w) *Carpinus* sp., PV. (x) *Corylus* sp., PV. (y) *Salix* sp., EV. (z–aa) *Geranium* sp., (z) PV, (aa) clavae detail.
Abbreviations: equatorial view (EV), polar view (PV), proximal view (PRV). Scale bars 10 µm (LM, e, g), 1 µm (c, k, m, o, q, aa).

Figure 5.

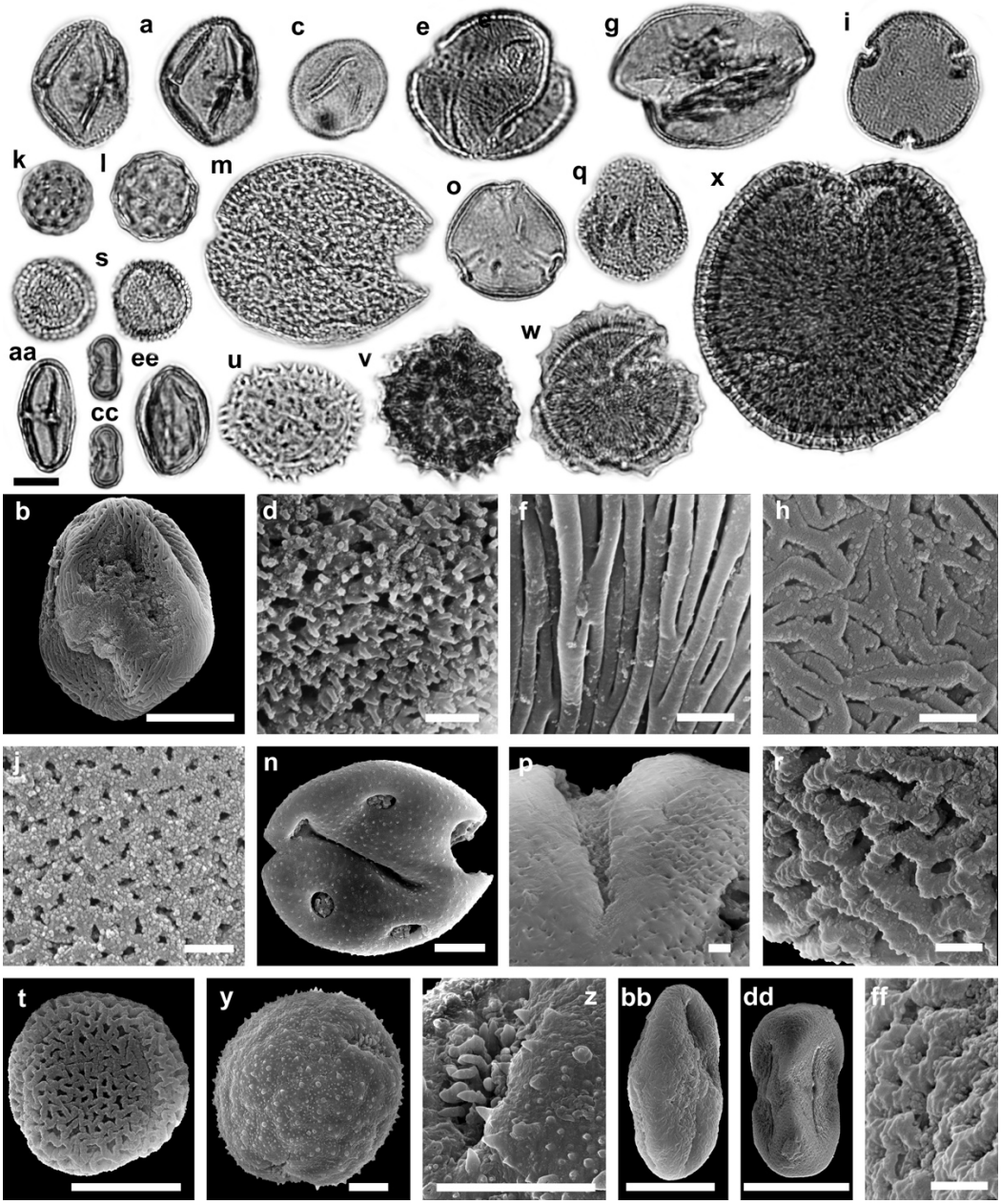

Figure 5. LM and SEM micrographs of Sapindales, Malvales, Caryophyllales, Cornales, Asterales, Dipsacales, and Apiales.
(a–b) *Cotinus* sp., EV. (c–d) *Pistacia* sp., (c) PV, (d) exine SEM detail. (e–f) *Acer* sp. 1, (e) PV, (f) mesocolpium SEM detail. (g–h) *Acer* sp. 2, (g) PV, (h) mesocolpium SEM detail. (i–j) *Craigia* sp., (i) PV, (j) apocolpium SEM detail. (k) Amaranthaceae/Chenopodioideae gen. indet. sp.1. (l) Amaranthaceae/Chenopodioideae gen. indet. sp.2. (m–n) Caryophyllaceae gen. indet. (o–p) *Nyssa* sp., (o) PV, (p) exine sculpturing and aperture SEM detail. (q–r) *Fraxinus* sp., (q) EV, (r) mesocolpium SEM detail. (s–t) *Olea* sp., EV. (u) Cichorioideae gen. indet., PV. (v) Asteraceae gen indet. sp. 1, PV. (w) Asteraceae gen indet. sp. 2, PV. (x–z) *Succisa* sp., (x–y) PV, (z) aperture SEM detail. (aa–bb) Apiaceae gen. indet. sp. 1, EV. (cc–dd) Apiaceae gen. indet. sp. 2, EV. (ee–ff) Angiosperm pollen fam. et gen. indet., (ee) EV, (ff) mesocolpium SEM detail.
Abbreviations: equatorial view (EV), polar view (PV). Scale bars 10 µm (LM, b, n, t, y, z, bb, dd), 1 µm (d, f, h, j, p, r, ff).

Figure 6.

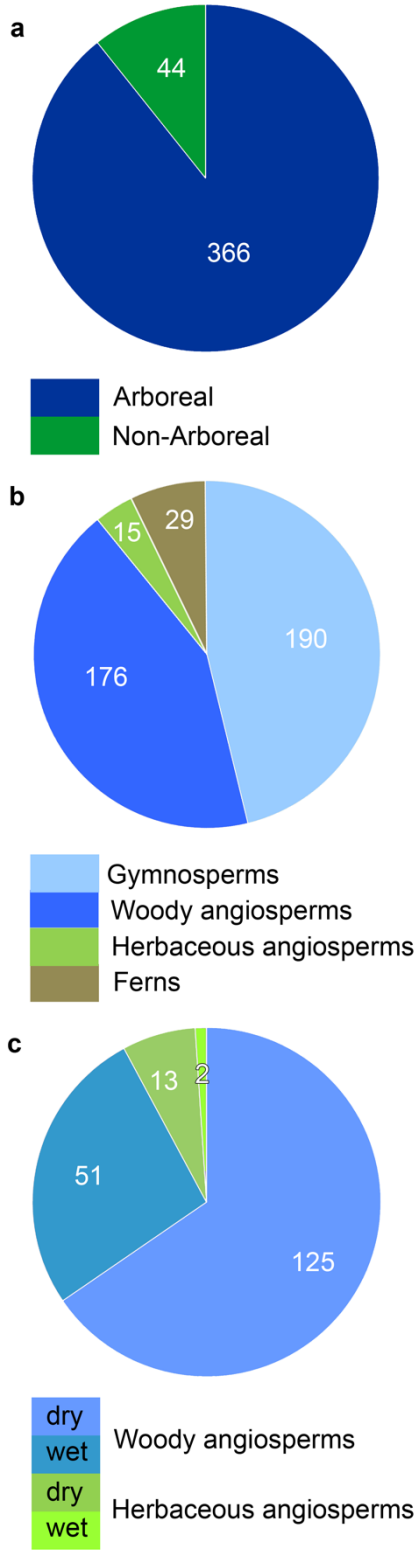

Figure 6. Palynomorph abundancies from sample S115992 based on 430 counted pollen and spores. Algae and unidentified angiosperm pollen excluded. (a) Ratio between pollen produced from arboreal and non-arboreal taxa. (b) Abundancies of woody gymnosperms and angiosperms and of herbaceous angiosperms and ferns. (c) Abundancy of woody and herbaceous angiosperms on dry and wet soils.

Figure 7.

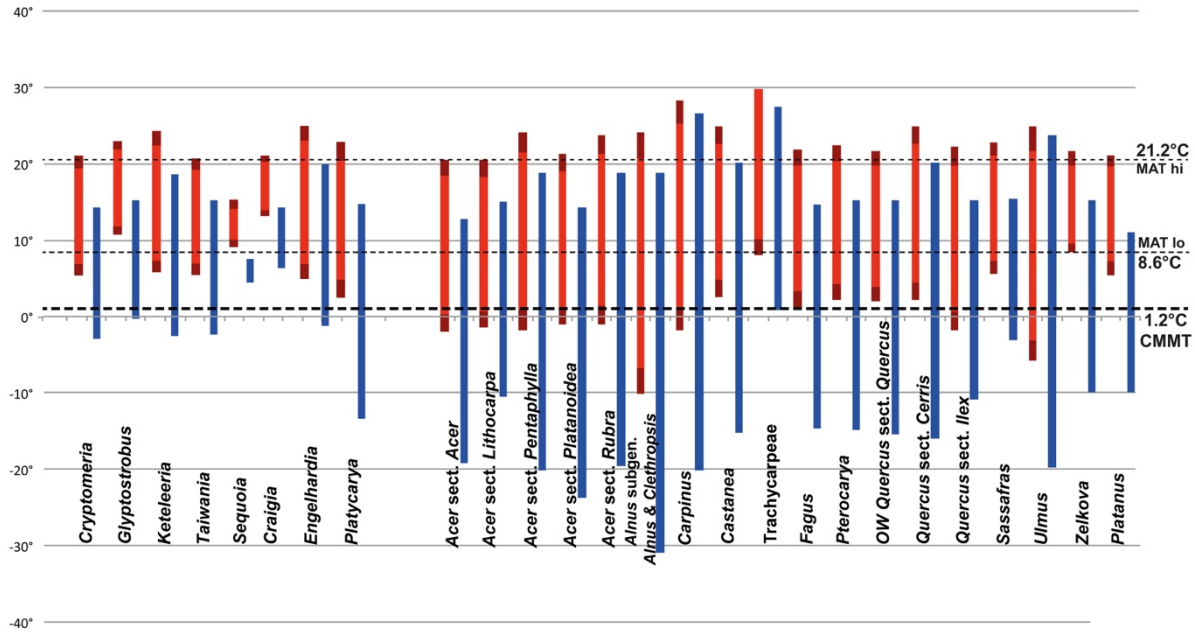

Figure 7. Coexistence-Approach diagram showing coexistence intervals for MAT and CMMT. MAT and CMMT climate ranges of relict taxa *a priori* excluded from the analysis are shown on the left side of the diagram.
Blue bars, coldest month mean temperature; red bars, 10–90 percentile climatic range (MAT); dark red extensions, full climatic range (MAT).

Fig. 8

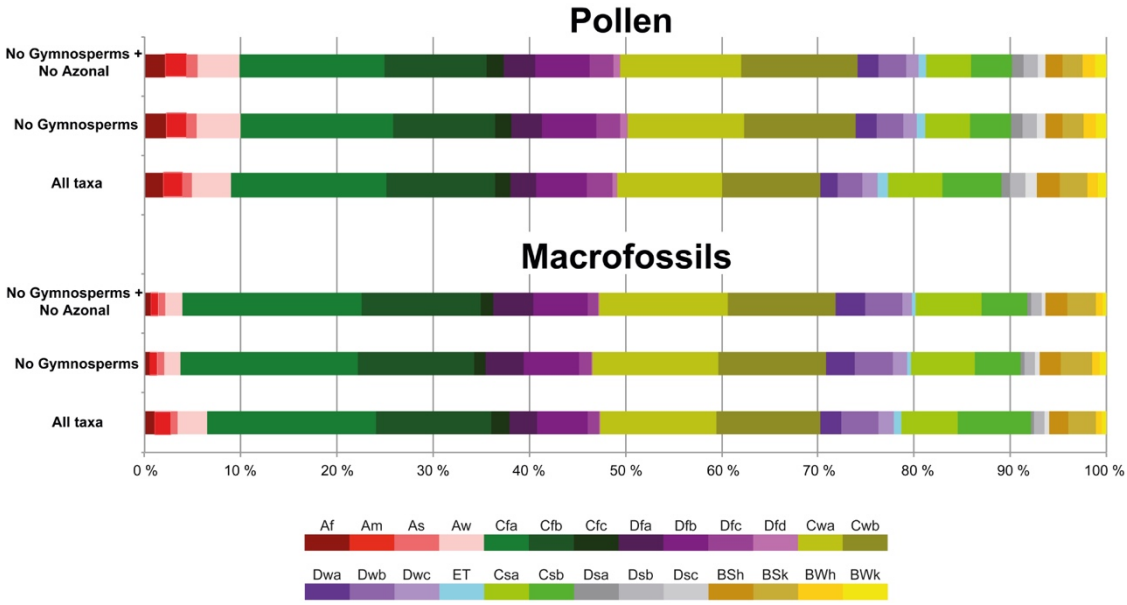

Figure 8. Köppen signal diagram for the macrofossil and pollen floras of Vegora.
To test and illustrate the stability of the climatic signal, gymnosperms (common alpine elements) and azonal elements (e.g. riparian or swamp vegetation) were excluded in some runs.